



**HAL**  
open science

## Rotation of a rigid satellite with a fluid component: a new light onto Titan's obliquity

Gwenaël Boué, Nicolas Rambaux, Andy Richard

► **To cite this version:**

Gwenaël Boué, Nicolas Rambaux, Andy Richard. Rotation of a rigid satellite with a fluid component: a new light onto Titan's obliquity. *Celestial Mechanics and Dynamical Astronomy*, 2017, 129 (4), pp.449 - 485. 10.1007/s10569-017-9790-8 . hal-01634864

**HAL Id: hal-01634864**

<https://hal.sorbonne-universite.fr/hal-01634864v1>

Submitted on 14 Nov 2017

**HAL** is a multi-disciplinary open access archive for the deposit and dissemination of scientific research documents, whether they are published or not. The documents may come from teaching and research institutions in France or abroad, or from public or private research centers.

L'archive ouverte pluridisciplinaire **HAL**, est destinée au dépôt et à la diffusion de documents scientifiques de niveau recherche, publiés ou non, émanant des établissements d'enseignement et de recherche français ou étrangers, des laboratoires publics ou privés.

# Rotation of a rigid satellite with a fluid component

## A new light onto Titan's obliquity

Gwenaël BOUÉ<sup>1</sup> · Nicolas RAMBAUX<sup>1</sup> ·  
Andy RICHARD<sup>1,2</sup>

Received: date / Accepted: date  
Version: September 21, 2017

**Abstract** We revisit the rotation dynamics of a rigid satellite with either a liquid core or a global sub-surface ocean. In both problems, the flow of the fluid component is assumed inviscid. The study of a hollow satellite with a liquid core is based on the Poincaré-Hough model which provides exact equations of motion. We introduce an approximation when the ellipticity of the cavity is low. This simplification allows to model both types of satellite in the same manner. The analysis of their rotation is done in a non-canonical Hamiltonian formalism closely related to Poincaré's "forme nouvelle des équations de la mécanique". In the case of a satellite with a global ocean, we obtain a seven-degree of freedom system. Six of them account for the motion of the two rigid components, and the last one is associated with the fluid layer. We apply our model to Titan for which the origin of the obliquity is still a debated question. We show that the observed value is compatible with Titan slightly departing from the hydrostatic equilibrium and being in a Cassini equilibrium state.

**Keywords** multi-layered body · spin-orbit coupling · Cassini state · synchronous rotation · analytical method · Io · Titan

### 1 Introduction

The spin pole of Titan, Saturn's largest moon, is lying close to the plane defined by its orbit pole and the Laplace pole (Stiles et al., 2008, 2010). This observation,

---

Gwenaël Boué  
E-mail: Gwenael.Boue@obspm.fr

Nicolas Rambaux  
E-mail: Nicolas.Rambaux@obspm.fr

Andy Richard  
E-mail: Andy.Richard@universcience.fr

<sup>1</sup> IMCCE, Observatoire de Paris, UPMC Univ. Paris 6, PSL Research University, Paris, France

<sup>2</sup> Universcience, Palais de la découverte, Paris, France

made by the RADAR instrument of the Cassini mission, suggests that Titan is in (or very close to) a Cassini state (Colombo, 1966; Peale, 1969). For a rigid body, the equilibrium obliquity is a function of its moments of inertia. Those of Titan have been deduced from its Stokes coefficients  $J_2 = (33.599 \pm 0.332) \times 10^{-6}$  and  $C_{22} = (10.121 \pm 0.029) \times 10^{-6}$  and from the hydrostatic equilibrium hypothesis implying a mean moment of inertia  $I/(mR^2) = 0.3431$  (Iess et al., 2012, SOL1a), where  $m$  and  $R$  are the mass and radius of Titan, respectively. The assumed hydrostatic equilibrium is suggested by the ratio  $J_2/C_{22} \approx 10/3$  which is precisely the expected value for a hydrostatic body (e.g., Rappaport et al., 1997). Assuming these values, if Titan were rigid and in a Cassini equilibrium state, its obliquity would be 0.113 deg (Bills and Nimmo, 2011), i.e. about one third of the radiometric value 0.32 deg (Stiles et al., 2008, 2010; Meriggiola et al., 2016). To match the observations, the frequency of the free libration in latitude must be reduced by a factor 0.526 (Bills and Nimmo, 2011). In particular, this would be the case if  $I/(mR^2)$  were increased to 0.45 (*ibid.*), a value exceeding  $2/5$  obtained for a homogeneous body, as if the mass of the satellite was concentrated toward the surface. This result leads to think that the observed obliquity is that of a thin shell partially decoupled from the interior by, e.g., a global ocean (*ibid.*).

The idea that the ice-covered satellites of the outer planets hold a global underneath ocean has already been proposed based on models of their internal structures (e.g., Lewis, 1971). Even the dwarf planet Pluto is suspected to harbour a subsurface ocean (Nimmo et al., 2016). In the case of Titan, the presence of the ocean is also revealed by laboratory experiments on the behaviour of water-ammonia compounds at high pressure and low temperature (Grasset and Sotin, 1996), by the detection of electromagnetic waves in its atmosphere (Béghin et al., 2012) and by the high value of its Love number  $k_2$  (Iess et al., 2012).

A dynamical problem closely related to the present one is that of a hollow satellite with a liquid core as described by the Poincaré-Hough model (Poincaré, 1910; Hough, 1895). For this specific problem, Poincaré (1901) developed a new Lagrangian formalism, based on the properties of the Lie group acting on the configuration space, which allows to derive the equations of motion in a very simple and elegant manner. Such a system is characterised by four degrees of freedom, three of them being associated with the rotation of the rigid mantle and the last one being due to the motion of the liquid core (e.g., Henrard, 2008). Applying this model to Jupiter’s satellite Io, Henrard (2008) observed that the frequency of the additional degree of freedom is close to the orbital frequency and should thus multiply the possibility of resonances. For Titan, we shall expect the same conclusion due to the presence of the ocean, but unfortunately, Poincaré’s model relies on the concept of a fluid simple motion which cannot be rigorously transposed to the case of a satellite with a global subsurface ocean.

In the case of Titan, the effect of an ocean on the rotation dynamics has been studied numerically using Euler’s rotation equations taking into account the gravitational interaction of Saturn on each layer, the pressure torques at the two fluid-solid boundaries, and the gravitational coupling between the interior and the shell (Baland et al., 2011, 2014; Noyelles and Nimmo, 2014). The elastic deformation of the solid layers and the atmospheric pressure have also been included in a modelling of the libration in longitude (Richard et al., 2014) and in a modelling of the Chandler polar motion (Coyette et al., 2016). Despite several arguments in favour of an ocean, this model does not easily explain the tilt of Titan’s spin-axis.

Indeed, under the hydrostatic equilibrium hypothesis, [Baland et al. \(2011\)](#) and [Noyelles and Nimmo \(2014\)](#) found that the obliquity of the Cassini state remains bounded below 0.15 deg, i.e. about one half of the observed value. There thus seemed to be a need for a significant resonant amplification to bring the system out of the Cassini equilibrium ([Baland et al., 2011](#); [Noyelles and Nimmo, 2014](#)). However these studies do not invoke the same mode as the origin of the resonant amplification. In addition, this solution does not agree with extended observations of the spin-axis orientation ([Meriggiola and Iess, 2012](#)). The model has then been amended to allow the Cassini state obliquity to reach the observed 0.32 deg, but this has only been made possible after releasing the hydrostatic shape assumption leaving the ratio  $J_2/C_{22} \approx 10/3$  unexplained ([Baland et al., 2014](#)).

It should be stressed that models developed thus far discard the rotation of the ocean relative to the inertial frame. This is a valid assumption to reproduce librations in longitude (e.g., [Richard, 2014](#)), but not anymore for precession motion. By consequence, the associated dynamical system only has 6 degrees of freedom equally shared by the rigid interior and the shell ([Noyelles and Nimmo, 2014](#)). Yet, a comparison of this problem with that of a satellite with a liquid core strongly suggests that a three layered body must have 7 degrees of freedom, one of which being brought by the ocean. Here, we aim at building a new dynamical model accounting for the rotation of the liquid layer as done by [Mathews et al. \(1991\)](#) for the Earth. More recently, the latter model has been adapted to the study of the Moon ([Dumberry and Wiczeorek, 2016](#))<sup>1</sup> and of Mercury ([Peale et al., 2016](#)). Here we reconsider the problem with a Hamiltonian approach. In that scope, we first extend the Lagrangian formalism described in ([Poincaré, 1901](#)) to a non-canonical Hamiltonian formalism allowing to study relative equilibria in a very efficient manner as in ([Maddocks, 1991](#); [Beck and Hall, 1998](#)). The method has proven its efficiency in the context of a rigid satellite in circular orbit ([Beck and Hall, 1998](#)), in the analysis of the two rigid body problem ([Maciejewski, 1995](#)), and in several studies of the attitude of a satellite with a gyrostat (e.g., [Hall and Beck, 2007](#); [Wang and Xu, 2012](#), and references therein). The approach is described in Sect. 2 and illustrated in the case of a rigid satellite in Sect. 3. We revisit the problem of a moon with a fluid core with this approach and we propose a simplification straightforwardly transposable to a three layered body in Sect. 4. The rotation dynamics of a satellite with a subsurface ocean is presented in Sect. 5. In the subsequent section 6, we test our model and our simplification on Io, a satellite with a liquid core, verifying that the derived eigenfrequencies are in very good agreement with those obtained in previous studies of the same problem made by [Noyelles \(2013, 2014\)](#). In this section, we also analyse the case of Titan showing that the additional degree of freedom makes the system highly sensitive to the internal structure and that the observed obliquity can be easily reproduced. Finally, we discuss our model and conclude in Sect. 7. The notation used in this paper is explained in Tab. 1.

---

<sup>1</sup> [Dumberry and Wiczeorek \(2016\)](#) could only highlight 5 degrees of freedom because their model of the Moon is axisymmetric and not triaxial.

## 2 Non-canonical Hamiltonian formalism

### 2.1 Equations of motion

#### 2.1.1 General case

Let a dynamical system with  $n$  degrees of freedom described by a Lagrangian  $L$ . We denote by  $Q$  the configuration space and each point  $\mathbf{q} \in Q$  is represented by a set of  $m \geq n$  coordinates  $(q_1, \dots, q_m)$ . The number of coordinates is purposely allowed to be greater than the actual dimension of the manifold  $Q$ . As in (Poincaré, 1901), we assume that there exists a transitive Lie group  $G$  acting on  $Q$ . The transitivity of  $G$  means that for all  $\mathbf{q}, \mathbf{q}' \in Q$ , there exists an element  $g$  of the group  $G$  such that  $\mathbf{q}' = g\mathbf{q}$ . In particular, given an initial condition  $\mathbf{q}_0$ , there exists  $g_t \in G$  such that the configuration  $\mathbf{q}(t)$  at time  $t$  reads  $\mathbf{q}(t) = g_t\mathbf{q}_0$ . In this work,  $G$  will be the rotation group  $SO(3)$ , the translation group  $T(3)$ , or some combinations of both.

Let  $\mathfrak{g}$  be the Lie algebra of  $G$ . By definition, there exists  $X \in \mathfrak{g}$  such that the generalised velocity reads  $\dot{\mathbf{q}} = X(\mathbf{q})$ . Since the action of  $G$  on  $Q$  is transitive, the dimension of  $\mathfrak{g}$  is equal to the number  $n$  of degrees of freedom. Let  $\mathcal{B} = (X_1, \dots, X_n)$  be a basis of  $\mathfrak{g}$  and  $(X_{ij})_{1 \leq i \leq n, 1 \leq j \leq m}$  be the  $n \times m$  functions of  $\mathbf{q}$  defined as

$$X_i = \sum_{j=1}^m X_{ij} \frac{\partial}{\partial q_j}. \quad (1)$$

We denote by  $\boldsymbol{\eta} = (\eta_1, \dots, \eta_n) \in \mathbb{R}^n$  the coordinates of  $X$  in  $\mathcal{B}$  such that

$$\dot{\mathbf{q}} = \sum_{i=1}^n \eta_i X_i(\mathbf{q}). \quad (2)$$

Because the term “generalised velocity” is already attributed to  $\dot{\mathbf{q}}$ , hereafter we call  $\boldsymbol{\eta}$  the *Lie velocity* of the system. Given two configurations  $\mathbf{q}$  and  $\mathbf{q}'$  infinitely closed to each other, we also define the  $n$ -tuple  $\delta \boldsymbol{\xi} = (\delta \xi_1, \dots, \delta \xi_n)$  such that

$$\delta \mathbf{q} := \mathbf{q}' - \mathbf{q} = \sum_{i=1}^n X_i(\mathbf{q}) \delta \xi_i. \quad (3)$$

Poincaré considers the Lagrangian as a function of  $(\boldsymbol{\eta}, \mathbf{q})$  and writes its infinitesimal variation as

$$\delta L = \sum_{i=1}^n \frac{\partial L}{\partial \eta_i} \delta \eta_i + X_i(L) \delta \xi_i. \quad (4)$$

The resulting equations of motion are (Poincaré, 1901)

$$\frac{d}{dt} \frac{\partial L}{\partial \eta_i} = \sum_{j,k} c_{ij}^k \eta_j \frac{\partial L}{\partial \eta_k} + X_i(L), \quad (5)$$

where  $c_{ij}^k$ , defined as

$$[X_i, X_j] := X_i X_j - X_j X_i = \sum_{k=1}^n c_{ij}^k X_k, \quad (6)$$

are the structure constants of  $\mathfrak{g}$  with respect to the chosen basis  $\mathcal{B}$ .

To get the Hamiltonian equations equivalent to Eq. (5), we introduce a momentum  $\boldsymbol{\pi}$  associated with the Lie velocity  $\boldsymbol{\eta}$ , and defined as

$$\boldsymbol{\pi} := \frac{\partial L}{\partial \boldsymbol{\eta}}. \quad (7)$$

Following the same nomenclature as for  $\boldsymbol{\eta}$ , we call this momentum  $\boldsymbol{\pi}$  the *Lie momentum* of the system. The Hamiltonian  $H$  is constructed by means of a Legendre transformation as

$$H(\boldsymbol{\pi}, \mathbf{q}) := \boldsymbol{\pi} \cdot \boldsymbol{\eta} - L(\boldsymbol{\eta}, \mathbf{q}). \quad (8)$$

Using Eqs. (4) and (7), the infinitesimal variation of  $H$  (Eq. 8) reads

$$\delta H = \sum_{i=1}^n \eta_i \delta \pi_i - X_i(L) \delta \xi_i. \quad (9)$$

But since  $H$  is a function of  $\boldsymbol{\pi}$  and  $\mathbf{q}$ , we also have, as in Eq. (4),

$$\delta H = \sum_{i=1}^n \frac{\partial H}{\partial \pi_i} \delta \pi_i + X_i(H) \delta \xi_i. \quad (10)$$

The identification of Eqs. (9) and (10) gives

$$\eta_i = \frac{\partial H}{\partial \pi_i} \quad \text{and} \quad X_i(H) = -X_i(L). \quad (11)$$

Using these identifications, the expression of  $\dot{\mathbf{q}}$  (Eq. 2), and Poincaré's equation (5) where  $\partial L / \partial \eta_i$  is replaced by  $\pi_i$  (Eq. 7), we get the non-canonical equations of motion associated with  $H$ , viz.,

$$\dot{q}_i = \sum_{j=1}^n \frac{\partial H}{\partial \pi_j} X_j(q_i) \quad \text{and} \quad \dot{\pi}_i = \sum_{j,k} c_{ij}^k \frac{\partial H}{\partial \pi_j} \pi_k - X_i(H). \quad (12)$$

Let us denote the state vector by  $\mathbf{y} = (\boldsymbol{\pi}, \mathbf{q}) \in \mathbb{R}^{n+m}$ . The equations of motion (12) written in matrix form read

$$\dot{\mathbf{y}} = -\mathbf{B}(\mathbf{y}) \nabla_{\mathbf{y}} H. \quad (13)$$

The so-called Poisson matrix  $\mathbf{B}(\mathbf{y})$  is

$$\mathbf{B}(\mathbf{y}) = \begin{bmatrix} \mathbf{C} & \mathbf{X} \\ -\mathbf{X}^T & \mathbf{0} \end{bmatrix} \quad (14)$$

where  $(\cdot)^T$  means the transpose of a vector or of a matrix.  $\mathbf{X}$  is an  $n \times m$  matrix and  $\mathbf{C}$  an  $n \times n$  matrix whose elements are

$$[\mathbf{X}]_{ij} = X_{ij} \quad \text{and} \quad [\mathbf{C}]_{ij} = -\sum_k c_{ij}^k \pi_k. \quad (15)$$

### 2.1.2 Translation group

The simplest illustration of the above formalism is the case where  $G$  is the translation group. In that case,  $\boldsymbol{\eta}$  is the usual velocity vector  $\mathbf{v}$  and  $\boldsymbol{\pi}$  is the standard linear momentum, commonly denoted  $\mathbf{p}$ . The vector fields of the tangent configuration space are  $X_i = \frac{\partial}{\partial q_i}$ . The associated structure constants  $c_{ij}^k$  are all nil. The Poisson matrix is then

$$\mathbf{B}(\mathbf{y}) = \begin{bmatrix} \mathbf{0} & \mathbf{1} \\ -\mathbf{1} & \mathbf{0} \end{bmatrix} \quad (16)$$

and we retrieve the canonical equations of motion

$$\dot{p}_i = -\frac{\partial H}{\partial q_i}, \quad \dot{q}_i = \frac{\partial H}{\partial p_i}. \quad (17)$$

### 2.1.3 Group $SO(3)$ in the body-fixed frame

The group  $SO(3)$  naturally appears in studies of the rotation motion of solid bodies. For this problem, two choices can be made: vectors are expressed either in the body-fixed frame or in the ‘‘laboratory’’ frame. Here, we consider the first option where vectors are written in the body-fixed frame. The Lie velocity is the rotation vector designated by  $\boldsymbol{\omega}$  and the orientation of the body is parametrised by the coordinates in the body-fixed frame of the laboratory base vectors, i.e.,  $\mathbf{q} = (\mathbf{i}, \mathbf{j}, \mathbf{k})$ . For any function  $f(\mathbf{i}, \mathbf{j}, \mathbf{k})$ , we have

$$\begin{aligned} \frac{d}{dt}f(\mathbf{i}, \mathbf{j}, \mathbf{k}) &= -(\boldsymbol{\omega} \times \mathbf{i}) \cdot \frac{\partial f}{\partial \mathbf{i}} - (\boldsymbol{\omega} \times \mathbf{j}) \cdot \frac{\partial f}{\partial \mathbf{j}} - (\boldsymbol{\omega} \times \mathbf{k}) \cdot \frac{\partial f}{\partial \mathbf{k}} \\ &= -\boldsymbol{\omega} \cdot \left( \mathbf{i} \times \frac{\partial f}{\partial \mathbf{i}} + \mathbf{j} \times \frac{\partial f}{\partial \mathbf{j}} + \mathbf{k} \times \frac{\partial f}{\partial \mathbf{k}} \right). \end{aligned} \quad (18)$$

Thus, the vector field  $X = (X_1, X_2, X_3)$  is

$$X = -\mathbf{i} \times \frac{\partial}{\partial \mathbf{i}} - \mathbf{j} \times \frac{\partial}{\partial \mathbf{j}} - \mathbf{k} \times \frac{\partial}{\partial \mathbf{k}}, \quad (19)$$

with structure constants  $c_{ij}^k = -\epsilon_{ijk}$  where  $\epsilon_{ijk} = 1$  when  $(i, j, k)$  is a cyclic permutation of  $(1, 2, 3)$ ,  $-1$  when  $(i, j, k)$  is a cyclic permutation of  $(3, 2, 1)$ ,  $0$  otherwise. Hence, the Poisson matrix reads

$$\mathbf{B} = - \begin{bmatrix} \hat{\boldsymbol{\pi}} & \hat{\mathbf{i}} & \hat{\mathbf{j}} & \hat{\mathbf{k}} \\ \hat{\mathbf{i}} & \mathbf{0} & \mathbf{0} & \mathbf{0} \\ \hat{\mathbf{j}} & \mathbf{0} & \mathbf{0} & \mathbf{0} \\ \hat{\mathbf{k}} & \mathbf{0} & \mathbf{0} & \mathbf{0} \end{bmatrix} \quad (20)$$

where for any vector  $\mathbf{v}$ , we have defined

$$\hat{\mathbf{v}} = \begin{bmatrix} 0 & -v_z & v_y \\ v_z & 0 & -v_x \\ -v_y & v_x & 0 \end{bmatrix}. \quad (21)$$

The corresponding equations of motion are

$$\frac{d\boldsymbol{\pi}}{dt} = \boldsymbol{\pi} \times \frac{\partial H}{\partial \boldsymbol{\pi}} + \mathbf{i} \times \frac{\partial H}{\partial \mathbf{i}} + \mathbf{j} \times \frac{\partial H}{\partial \mathbf{j}} + \mathbf{k} \times \frac{\partial H}{\partial \mathbf{k}}, \quad (22)$$

$$\frac{d\mathbf{i}}{dt} = \mathbf{i} \times \frac{\partial H}{\partial \boldsymbol{\pi}}, \quad (23)$$

$$\frac{d\mathbf{j}}{dt} = \mathbf{j} \times \frac{\partial H}{\partial \boldsymbol{\pi}}, \quad (24)$$

$$\frac{d\mathbf{k}}{dt} = \mathbf{k} \times \frac{\partial H}{\partial \boldsymbol{\pi}} \quad (25)$$

with  $\partial H / \partial \boldsymbol{\pi} = \boldsymbol{\omega}$ .

#### 2.1.4 Group $SO(3)$ in the laboratory frame

Here we again consider the rotation motion of a solid body but now vector coordinates are written in the laboratory frame. The latter is the frame with respect to which the motion of the spinning body is described. Note that it does not have to be inertial. The generalised coordinates are the base vectors of the rotated frame  $\mathbf{q} = (\mathbf{I}, \mathbf{J}, \mathbf{K})$  and the Lie momentum associated with the rotation vector is denoted  $\boldsymbol{\Pi}$ . Applying the same method as above, we get

$$X = \mathbf{I} \times \frac{\partial}{\partial \mathbf{I}} + \mathbf{J} \times \frac{\partial}{\partial \mathbf{J}} + \mathbf{K} \times \frac{\partial}{\partial \mathbf{K}}. \quad (26)$$

For this basis, the structure constants are  $c_{ij}^k = \epsilon_{ijk}$  and thus, the Poisson matrix is

$$\mathbf{B} = \begin{bmatrix} \hat{\boldsymbol{\Pi}} & \hat{\mathbf{I}} & \hat{\mathbf{J}} & \hat{\mathbf{K}} \\ \hat{\mathbf{I}} & \mathbf{0} & \mathbf{0} & \mathbf{0} \\ \hat{\mathbf{J}} & \mathbf{0} & \mathbf{0} & \mathbf{0} \\ \hat{\mathbf{K}} & \mathbf{0} & \mathbf{0} & \mathbf{0} \end{bmatrix}. \quad (27)$$

The associated equations of motion are

$$\frac{d\boldsymbol{\Pi}}{dt} = \frac{\partial H}{\partial \boldsymbol{\Pi}} \times \boldsymbol{\Pi} + \frac{\partial H}{\partial \mathbf{I}} \times \mathbf{I} + \frac{\partial H}{\partial \mathbf{J}} \times \mathbf{J} + \frac{\partial H}{\partial \mathbf{K}} \times \mathbf{K}, \quad (28)$$

$$\frac{d\mathbf{I}}{dt} = \frac{\partial H}{\partial \boldsymbol{\Pi}} \times \mathbf{I}, \quad (29)$$

$$\frac{d\mathbf{J}}{dt} = \frac{\partial H}{\partial \boldsymbol{\Pi}} \times \mathbf{J}, \quad (30)$$

$$\frac{d\mathbf{K}}{dt} = \frac{\partial H}{\partial \boldsymbol{\Pi}} \times \mathbf{K} \quad (31)$$

where  $\partial H / \partial \boldsymbol{\Pi}$  still is the rotation vector, although expressed in the laboratory frame.



## 2.2 Linearisation and driven solution

For the sake of completeness, we here recall the general method leading to the linearisation of the equations of motion in the non-canonical Hamiltonian formalism (Maddocks, 1991; Beck and Hall, 1998). We also present the criterion of nonlinear stability as described in *ibid*.

Let a non-autonomous Hamiltonian  $H(\mathbf{y}, t)$  associated with an  $n$  degrees of freedom system expressed as a function of non-canonical variables  $\mathbf{y} \in \mathbb{R}^p$  with  $p \geq 2n$ . We assume that  $H(\mathbf{y}, t)$  can be split as follows

$$H(\mathbf{y}, t) = H_0(\mathbf{y}) + H_1(\mathbf{y}, t), \quad (32)$$

where  $H_0(\mathbf{y})$  is the autonomous part of  $H(\mathbf{y}, t)$  and  $H_1(\mathbf{y}, t)$  a small perturbation. Let us skip the perturbation  $H_1$  for a moment. The equations of motion associated with  $H_0(\mathbf{y})$  are of the form

$$\dot{\mathbf{y}} = -\mathbf{B}(\mathbf{y})\nabla_{\mathbf{y}}H_0(\mathbf{y}). \quad (33)$$

The system has  $n$  degrees of freedom, its phase space  $\Sigma$  is thus a manifold of dimension  $2n$ . Since  $\mathbf{y} \in \mathbb{R}^p$ , there exists  $s = p - 2n$  Casimir functions  $C_i(\mathbf{y})$  and  $s$  constants  $c_i$ ,  $1 \leq i \leq s$ , such that

$$\Sigma = \{\mathbf{y} \in \mathbb{R}^p : C_1(\mathbf{y}) = c_1, \dots, C_s(\mathbf{y}) = c_s\}. \quad (34)$$

We recall that Casimir functions are constants of the motion for any Hamiltonian because their gradients constitute a basis of the kernel of the Poisson matrix:

$$\ker \mathbf{B}(\mathbf{y}) = \text{span} \{\nabla_{\mathbf{y}}C_1(\mathbf{y}), \dots, \nabla_{\mathbf{y}}C_s(\mathbf{y})\}, \quad (35)$$

and thus

$$\dot{C}_i(\mathbf{y}) = (\nabla_{\mathbf{y}}H_0)^{\text{T}}\mathbf{B}(\mathbf{y})\nabla_{\mathbf{y}}C_i = 0 \quad (36)$$

for all Hamiltonian  $H_0$ .

Let  $\mathbf{y}_e$  be an equilibrium, i.e., a fixed point of  $H_0$ . According to Eq. (33),  $\dot{\mathbf{y}}_e = \mathbf{0}$  implies  $\nabla_{\mathbf{y}}H_0(\mathbf{y}_e) \in \ker \mathbf{B}(\mathbf{y}_e)$ . Thus, there exists  $s$  coefficients  $(\mu_i)_{1 \leq i \leq s}$  such that

$$\nabla_{\mathbf{y}}H_0(\mathbf{y}_e) = \sum_{i=1}^s \mu_i \nabla_{\mathbf{y}}C_i(\mathbf{y}_e). \quad (37)$$

Let

$$F(\mathbf{y}) = H_0(\mathbf{y}) - \sum_{i=1}^s \mu_i C_i(\mathbf{y}). \quad (38)$$

By construction,  $F$  satisfies  $\nabla_{\mathbf{y}}F(\mathbf{y}_e) = \mathbf{0}$ . Coefficients  $\mu_i$  can be seen as Lagrange multipliers and functions  $C_i(\mathbf{y})$  as constraints since we search for an extremum of  $H_0(\mathbf{y})$  under the conditions  $C_i(\mathbf{y}) = c_i$ . The  $p + s$  equations  $\nabla_{\mathbf{y}}F(\mathbf{y}_e) = \mathbf{0}$  and  $C_i(\mathbf{y}_e) = c_i$  allow to determine  $\mathbf{y}_e$  and the coefficients  $\mu_i$ .

Once  $\mathbf{y}_e$  and coefficients  $\mu_i$  are known, the linearisation of the equations of motion (Eq. 33) are given by

$$\delta\dot{\mathbf{y}} = \mathbf{A}(\mathbf{y}_e)\delta\mathbf{y} \quad (39)$$

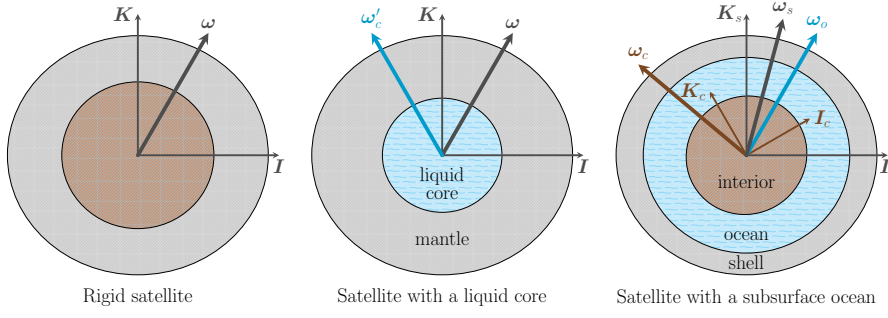


**Fig. 1** Rigid satellites are characterised by their basis vectors  $(\mathbf{I}, \mathbf{J}, \mathbf{K})$  and their rotation vector  $\boldsymbol{\omega}$  with respect to the laboratory frame. The same vectors are used for satellites with a liquid core, but the angular speed  $\boldsymbol{\omega}'_c$  of the core with respect to the mantle is also specified. In the case of a satellite with a global ocean, all vectors are expressed in the laboratory frame. These are the basis vectors of the shell  $(\mathbf{I}_s, \mathbf{J}_s, \mathbf{K}_s)$  and of the interior  $(\mathbf{I}_c, \mathbf{J}_c, \mathbf{K}_c)$ , and the rotation vectors  $\boldsymbol{\omega}_c, \boldsymbol{\omega}_o, \boldsymbol{\omega}_s$  associated with the central region, the ocean and the shell, respectively.

with  $\delta\mathbf{y} = \mathbf{y} - \mathbf{y}_e$  and (Maddocks, 1991)

$$\mathbf{A}(\mathbf{y}_e) = -\mathbf{B}(\mathbf{y}_e)\nabla_{\mathbf{y}}^2 F(\mathbf{y}_e). \quad (40)$$

In a last step, the perturbation  $H_1(\mathbf{y}, t)$  is taken into account and the equations of motion become

$$\delta\dot{\mathbf{y}} - \mathbf{A}(\mathbf{y}_e)\delta\mathbf{y} = \mathbf{z}(t), \quad (41)$$

with

$$\mathbf{z}(t) = -\mathbf{B}(\mathbf{y}_e)\nabla_{\mathbf{y}} H_1(\mathbf{y}_e, t). \quad (42)$$

Equation (41) is then solved using standard techniques.

The relative equilibria  $\mathbf{y} = \mathbf{y}_e$  is said to be nonlinearly stable if the quadratic form (or Lyapunov function)  $N(\mathbf{y}) = \mathbf{y}^T \mathbf{N} \mathbf{y}$ , defined on the phase space  $\Sigma$  by its Hessian (below), is a strictly convex function (Beck and Hall, 1998). The Hessian of  $N(\mathbf{y})$  is given by (see *ibid.*)

$$\mathbf{N} := \nabla^2 N = \mathbf{Q}(\mathbf{y}_e)\nabla^2 F(\mathbf{y}_e)\mathbf{Q}(\mathbf{y}_e), \quad (43)$$

where  $\mathbf{Q}(\mathbf{y})$  is the orthogonal projection matrix onto the range of  $\mathbf{A}(\mathbf{y})$ ,

$$\mathbf{Q}(\mathbf{y}) = \mathbf{1} - \mathbf{K}(\mathbf{y})(\mathbf{K}^T(\mathbf{y})\mathbf{K}(\mathbf{y}))^{-1}\mathbf{K}^T(\mathbf{y}), \quad (44)$$

and where  $\mathbf{K}(\mathbf{y})$  is a  $p \times s$  matrix given by

$$\mathbf{K}(\mathbf{y}) = [\nabla C_1(\mathbf{y}) \cdots \nabla C_s(\mathbf{y})]. \quad (45)$$

**Table 1** Notations

symbol	definition
$c, o, m, s$	indices standing for Core, Ocean, Mantle, and Shell, respectively
$rs, fc, go$	indices standing for Rigid Satellite, Fluid Core, and Global Ocean
$\mathcal{F}_{in} = (\mathbf{i}_0, \mathbf{j}_0, \mathbf{k}_0)$	inertial frame
$\mathcal{F}_{lab} = (\mathbf{i}, \mathbf{j}, \mathbf{k})$	laboratory frame
$\mathcal{F}_i = (\mathbf{I}_i, \mathbf{J}_i, \mathbf{K}_i)$	frame associated with the layer $i$
$\Omega$	rotation vector of $\mathcal{F}_{lab}$ with respect to $\mathcal{F}_{in}$ expressed in $\mathcal{F}_{lab}$
$\omega_i$	rotation vector of $\mathcal{F}_i$ with respect to $\mathcal{F}_{lab}$ expressed in $\mathcal{F}_{lab}$
$\omega'_c$	rotation vector of $\mathcal{F}_c$ with respect to $\mathcal{F}_m$ expressed in $\mathcal{F}_m$
$\Pi_i$	Lie momentum associated with $\omega_i$
$\Pi'_c$	Lie momentum associated with $\omega'_c$
$\mathbf{I}_i, \mathbf{J}_i, \mathbf{K}_i$	basis vectors of $\mathcal{F}_i$ expressed in $\mathcal{F}_{lab}$
$\mathbf{R}_i = [\mathbf{I}_i, \mathbf{J}_i, \mathbf{K}_i]$	rotation matrix of the layer $i$ relative to $\mathcal{F}_{lab}$
$\mathbf{y}_i = (\Pi_i, \mathbf{I}_i, \mathbf{J}_i, \mathbf{K}_i)$	state vector of the layer $i$
$\mathbf{y}$	state vector of the whole system
$T(\mathbf{y})$	kinetic energy
$U(\mathbf{y}, t)$	potential energy
$L(\mathbf{y}, t)$	Lagrangian
$H(\mathbf{y}, t)$	Hamiltonian
$C_i(\mathbf{y})$	Casimir functions
$\mu_i$	Lagrange multipliers
$F(\mathbf{y})$	Lagrangian associated with the minimisation of $H_0$ with constraints
$\mathbf{B}(\mathbf{y})$	Poisson matrix
$\mathbf{A}(\mathbf{y})$	matrix of the linearised system
$U_0(\mathbf{y})$	constant part of $U(\mathbf{y}, t)$
$U_1(\mathbf{y}, t)$	perturbation $U(\mathbf{y}, t) - U_0(\mathbf{y})$
$U_{self}(\mathbf{y})$	self gravitational energy of the satellite
$(u_{ij})_{i,j \in \{x,y,z\}}$	constant parameters of $U_{self}$
$H_0(\mathbf{y})$	autonomous part of $H(\mathbf{y}, t)$
$H_1(\mathbf{y}, t)$	perturbation $H(\mathbf{y}, t) - H_0(\mathbf{y})$
$\mathbf{r}, \mathbf{r}(t)$	radius vector connecting the satellite barycenter to the planet
$\mathbf{S}(t)$	$\mathcal{G}M_p \mathbf{r} \mathbf{r}^T / r^5$
$\mathbf{S}_0$	constant part of $\mathbf{S}(t)$
$\mathbf{S}_1(t)$	$\mathbf{S}(t) - \mathbf{S}_0$
$(\sigma_{uv}^0)_{u,v \in \{x,y,z\}}$	elements of the matrix $\mathbf{S}_0$
$(\sigma_{uv}^1(t))_{u,v \in \{x,y,z\}}$	elements of the matrix $\mathbf{S}_1(t)$
$\mathcal{G}$	gravitational constant
$M_p$	mass of the central planet
$\alpha_i, \beta_i, \gamma_i$	$(C_i - B_i)/A_i, (C_i - A_i)/B_i, (B_i - A_i)/C_i$ , respectively
$\rho_i$	density of the layer $i$
$a_i, b_i, c_i$	radii of the outer boundary of the layer $i$
$\zeta$	equatorial flattening $(a - b)/a$
$\mathbb{I}_i$	inertia tensor of the layer $i$ expressed in $\mathcal{F}_{lab}$
$\mathbb{I}'$	ancillary inertia tensor
$A_i, B_i, C_i$	principal moments of inertia of the layer $i$
$A', B', C'$	ancillary moments of inertia
$\omega_u$	frequency of libration in longitude
$\omega_v$	frequency of libration in latitude
$\omega_w$	wobble frequency

### 3 Rigid satellite

Let a rigid satellite whose rotation is close to the synchronous state, i.e., whose mean rotation rate is equal to the orbital mean motion. The goal of this section is to compute the frequencies associated with the free modes of rotation, to evaluate the forced obliquity driven by the orbital precession, and eventually to check the nonlinear stability of the system in the vicinity of the equilibrium. The analysis is performed using the non-canonical Hamiltonian formalism described in Sect. 2. It turns out to be convenient to describe the problem in a laboratory frame rotating at constant angular speed  $\boldsymbol{\Omega}$  with respect to the inertial frame.  $\boldsymbol{\Omega}$  will then be chosen equal to the mean orbital motion. We denote by  $\boldsymbol{\omega}$  the rotation vector of the satellite with respect to the laboratory frame  $\mathcal{F}_{\text{lab}}$  and by  $(\mathbf{I}, \mathbf{J}, \mathbf{K})$  its principal axes of inertia such that the matrix of inertia reads

$$\mathbb{I} = \mathbf{R} \text{diag}(A, B, C) \mathbf{R}^T, \quad (46)$$

where  $\mathbf{R} = [\mathbf{I}, \mathbf{J}, \mathbf{K}]$  is the rotation matrix of the satellite with respect to the laboratory frame and where  $(.)^T$  denotes the transpose operator. Note that the matrix of inertia can also be written in a equivalent form facilitating the computation of the gradient of the forthcoming Hamiltonian

$$\mathbb{I} = A\mathbf{I}\mathbf{I}^T + B\mathbf{J}\mathbf{J}^T + C\mathbf{K}\mathbf{K}^T. \quad (47)$$

The Lie velocity of the system is thus  $\boldsymbol{\omega}$  while  $(\mathbf{I}, \mathbf{J}, \mathbf{K})$  are the generalised coordinates. We also denote by  $(\mathbf{i}, \mathbf{j}, \mathbf{k})$  the basis vectors associated with the laboratory frame. The radius vector connecting the planet and the satellite barycenter is assumed to be a known function of time and is denoted either by  $\mathbf{r}(t)$  or simply by  $\mathbf{r}$ .  $\mathcal{G}$  and  $M_p$  are the gravitational constant and the mass of the planet, respectively. With these notations, the (non-autonomous) Lagrangian  $L_{\text{rs}}(\boldsymbol{\omega}, \mathbf{I}, \mathbf{J}, \mathbf{K}, t)$  governing the rotation of the rigid satellite is

$$L_{\text{rs}}(\boldsymbol{\omega}, \mathbf{I}, \mathbf{J}, \mathbf{K}, t) = \frac{(\boldsymbol{\omega} + \boldsymbol{\Omega})^T \mathbb{I} (\boldsymbol{\omega} + \boldsymbol{\Omega})}{2} - \frac{3\mathcal{G}M_p}{2} \frac{\mathbf{r}^T \mathbb{I} \mathbf{r}}{r^5}. \quad (48)$$

The Lie momentum  $\boldsymbol{\Pi}$  associated with  $\boldsymbol{\omega}$  reads

$$\boldsymbol{\Pi} = \frac{\partial L_{\text{rs}}}{\partial \boldsymbol{\omega}} = \mathbb{I}(\boldsymbol{\omega} + \boldsymbol{\Omega}). \quad (49)$$

We recognise the spin angular momentum of the satellite with respect to the inertial frame and expressed in the laboratory frame. The Hamiltonian  $H_{\text{rs}}(\boldsymbol{\Pi}, \mathbf{I}, \mathbf{J}, \mathbf{K}, t)$  resulting from the Legendre transformation applied to  $L_{\text{rs}}(\boldsymbol{\omega}, \mathbf{I}, \mathbf{J}, \mathbf{K}, t)$  reads

$$H_{\text{rs}}(\boldsymbol{\Pi}, \mathbf{I}, \mathbf{J}, \mathbf{K}, t) = \frac{\boldsymbol{\Pi}^T \mathbb{I}^{-1} \boldsymbol{\Pi}}{2} - \boldsymbol{\Omega}^T \boldsymbol{\Pi} + \frac{3\mathcal{G}M_p}{2} \frac{\mathbf{r}^T \mathbb{I} \mathbf{r}}{r^5} \quad (50)$$

with

$$\mathbb{I}^{-1} = \frac{\mathbf{I}\mathbf{I}^T}{A} + \frac{\mathbf{J}\mathbf{J}^T}{B} + \frac{\mathbf{K}\mathbf{K}^T}{C}. \quad (51)$$

The Poisson matrix  $\mathbf{B}_{\text{rs}}(\mathbf{y})$  associated with  $\mathbf{y} = (\mathbf{\Pi}, \mathbf{I}, \mathbf{J}, \mathbf{K})$  is the one given in Eq. (27). The gradient of the Hamiltonian reads

$$\frac{\partial H_{\text{rs}}}{\partial \mathbf{\Pi}} = \mathbb{I}^{-1} \mathbf{\Pi} - \mathbf{\Omega} = \boldsymbol{\omega}, \quad (52)$$

$$\frac{\partial H_{\text{rs}}}{\partial \mathbf{I}} = \frac{(\mathbf{I} \cdot \mathbf{\Pi})}{A} \mathbf{\Pi} + 3 \frac{\mathcal{G}M_p}{r^5} A (\mathbf{r} \cdot \mathbf{I}) \mathbf{r}, \quad (53)$$

$$\frac{\partial H_{\text{rs}}}{\partial \mathbf{J}} = \frac{(\mathbf{J} \cdot \mathbf{\Pi})}{B} \mathbf{\Pi} + 3 \frac{\mathcal{G}M_p}{r^5} B (\mathbf{r} \cdot \mathbf{J}) \mathbf{r}, \quad (54)$$

$$\frac{\partial H_{\text{rs}}}{\partial \mathbf{K}} = \frac{(\mathbf{K} \cdot \mathbf{\Pi})}{C} \mathbf{\Pi} + 3 \frac{\mathcal{G}M_p}{r^5} C (\mathbf{r} \cdot \mathbf{K}) \mathbf{r}, \quad (55)$$

and thus the equations of motion are

$$\dot{\mathbf{\Pi}} = \mathbf{\Pi} \times \mathbf{\Omega} - 3 \frac{\mathcal{G}M_p}{r^5} (\mathbb{I} \mathbf{r}) \times \mathbf{r}, \quad (56)$$

$$\dot{\mathbf{I}} = \boldsymbol{\omega} \times \mathbf{I}, \quad (57)$$

$$\dot{\mathbf{J}} = \boldsymbol{\omega} \times \mathbf{J}, \quad (58)$$

$$\dot{\mathbf{K}} = \boldsymbol{\omega} \times \mathbf{K}. \quad (59)$$

Equations of motion (Eqs. 56-59) are those of the full Hamiltonian. Because  $\mathbf{r}(t)$  is a function of time, the set of equations (56-59) has no fixed point. To proceed, we set  $\mathbf{\Omega} = \Omega \mathbf{k}$  with  $\Omega$  equal to the mean orbital motion such that, in the laboratory frame  $(\mathbf{i}, \mathbf{j}, \mathbf{k})$ ,

$$\mathbf{S}(t) := \mathcal{G}M_p \frac{\mathbf{r} \mathbf{r}^T}{r^5} = \mathbf{S}_0 + \mathbf{S}_1(t) \quad (60)$$

where  $\mathbf{S}_0$  is a constant matrix and  $\mathbf{S}_1(t)$  a small perturbation. Furthermore, the initial angle of the rotation is chosen such that  $\mathbf{S}_0$  is diagonal with components  $(\sigma_{xx}^0, \sigma_{yy}^0, \sigma_{zz}^0)$ . Similarly, we denote by  $\sigma_{uv}^1$ , where  $u, v \in \{x, y, z\}$ , the elements of  $\mathbf{S}_1(t)$ . The gravitational potential energy  $U(\mathbf{y}, t)$  is then split into  $U_0(\mathbf{y}) + U_1(\mathbf{y}, t)$  with

$$U_0(\mathbf{y}) = \frac{3}{2} \left( A \mathbf{I}^T \mathbf{S}_0 \mathbf{I} + B \mathbf{J}^T \mathbf{S}_0 \mathbf{J} + C \mathbf{K}^T \mathbf{S}_0 \mathbf{K} \right), \quad (61)$$

$$U_1(\mathbf{y}, t) = \frac{3}{2} \left( A \mathbf{I}^T \mathbf{S}_1(t) \mathbf{I} + B \mathbf{J}^T \mathbf{S}_1(t) \mathbf{J} + C \mathbf{K}^T \mathbf{S}_1(t) \mathbf{K} \right). \quad (62)$$

As a result, the Hamiltonian  $H_{\text{rs}}(\mathbf{y}, t)$  also get split into  $H_{\text{rs}}^0(\mathbf{y}) + H_{\text{rs}}^1(\mathbf{y}, t)$  with

$$H_{\text{rs}}^0(\mathbf{y}) = \frac{\mathbf{\Pi}^T \mathbb{I}^{-1} \mathbf{\Pi}}{2} - \mathbf{\Omega}^T \mathbf{\Pi} + U_0(\mathbf{y}), \quad (63)$$

$$H_{\text{rs}}^1(\mathbf{y}, t) = U_1(\mathbf{y}, t). \quad (64)$$

In the case of a Keplerian orbit with eccentricity  $e$  and inclination  $i$  with respect to the reference frame,

$$\sigma_{xx}^0 = \frac{\mathcal{G}M_p}{a^3} \left( \frac{X_0^{-3,0}(e) + X_2^{-3,2}(e)}{2} \cos^4 \left( \frac{i}{2} \right) + \frac{X_0^{-3,0}(e)}{2} \sin^4 \left( \frac{i}{2} \right) \right), \quad (65)$$

$$\sigma_{yy}^0 = \frac{\mathcal{G}M_p}{a^3} \left( \frac{X_0^{-3,0}(e) - X_2^{-3,2}(e)}{2} \cos^4 \left( \frac{i}{2} \right) + \frac{X_0^{-3,0}(e)}{2} \sin^4 \left( \frac{i}{2} \right) \right), \quad (66)$$

$$\sigma_{zz}^0 = \frac{\mathcal{G}M_p}{a^3} \frac{X_0^{-3,0}(e)}{2} \sin^2 i, \quad (67)$$

where  $X_k^{n,m}(e)$  are Hansen coefficients (Hansen, 1855) defined as Fourier coefficients of the series

$$\left(\frac{r}{a}\right)^n e^{imv} = \sum_{k=-\infty}^{\infty} X_k^{n,m}(e) e^{ikM} \quad (68)$$

with  $a$ ,  $v$ ,  $M$  being the semimajor axis, the true anomaly and the mean anomaly, respectively. Besides, in this study a single element of the matrix  $\mathbf{S}_1(t)$  plays a role in the tilting of the Cassini state, this is the term in  $\sigma_{xz}^1(t) = \sigma_{zx}^1(t)$  corresponding to the first harmonic of the orbital precession in inclination whose expression is

$$\sigma_{xz}^1(t) = \frac{\mathcal{G}M_p}{a^3} \left( \frac{X_0^{-3,0}(e)}{2} \cos i + \frac{X_2^{-3,2}(e)}{2} \cos^2 \frac{i}{2} \right) \sin i \sin(\Omega t - \Phi) \quad (69)$$

where  $\Phi$  is the longitude of the ascending node. The expression of the Hansen coefficients involved in  $\mathbf{S}_0$  and  $\mathbf{S}_1(t)$  are

$$X_0^{-3,0}(e) = (1 - e^2)^{-3/2}, \quad (70)$$

$$X_2^{-3,2}(e) = 1 - \frac{5}{2}e^2 + \frac{13}{16}e^4 - \frac{35}{288}e^6 + O(e^8). \quad (71)$$

Following the steps recalled in the previous section 2.2, we now skip the perturbation  $\mathbf{S}_1(t)$  for a while and only retain the autonomous part of the Hamiltonian  $H_{\text{rs}}^0(\mathbf{y})$ . The gradient of the Hamiltonian  $H_{\text{rs}}^0(\mathbf{y})$  reads

$$\frac{\partial H_{\text{rs}}^0}{\partial \mathbf{\Pi}} = \mathbb{I}^{-1} \mathbf{\Pi} - \mathbf{\Omega} = \boldsymbol{\omega}, \quad (72)$$

$$\frac{\partial H_{\text{rs}}^0}{\partial \mathbf{I}} = \frac{(\mathbf{I} \cdot \mathbf{\Pi})}{A} \mathbf{\Pi} + 3A \mathbf{S}_0 \mathbf{I}, \quad (73)$$

$$\frac{\partial H_{\text{rs}}^0}{\partial \mathbf{J}} = \frac{(\mathbf{J} \cdot \mathbf{\Pi})}{B} \mathbf{\Pi} + 3B \mathbf{S}_0 \mathbf{J}, \quad (74)$$

$$\frac{\partial H_{\text{rs}}^0}{\partial \mathbf{K}} = \frac{(\mathbf{K} \cdot \mathbf{\Pi})}{C} \mathbf{\Pi} + 3C \mathbf{S}_0 \mathbf{K}. \quad (75)$$

Only  $\dot{\mathbf{\Pi}}$  (Eq. 56) is affected by the averaging process. Its new equation of motion reads

$$\dot{\mathbf{\Pi}} = \mathbf{\Pi} \times \mathbf{\Omega} + 3A(\mathbf{S}_0 \mathbf{I}) \times \mathbf{I} + 3B(\mathbf{S}_0 \mathbf{J}) \times \mathbf{J} + 3C(\mathbf{S}_0 \mathbf{K}) \times \mathbf{K}. \quad (76)$$

### 3.1 Linearisation

To perform the linearisation of Eqs. (76, 57-59), we note that the phase space  $\Sigma_{\text{rs}}$  of the system is a manifold of dimension 6 (associated with the 3 degrees of freedom of the group  $\text{SO}(3)$ ) defined as

$$\Sigma_{\text{rs}} = \{\mathbf{y} \in \mathbb{R}^{12} : C_{\text{rs}}^1(\mathbf{y}) = C_{\text{rs}}^2(\mathbf{y}) = C_{\text{rs}}^3(\mathbf{y}) = 1/2, \\ C_{\text{rs}}^4(\mathbf{y}) = C_{\text{rs}}^5(\mathbf{y}) = C_{\text{rs}}^6(\mathbf{y}) = 0\}, \quad (77)$$

where the Casimir functions are

$$C_{\text{rs}}^1(\mathbf{y}) = \frac{1}{2} \mathbf{I} \cdot \mathbf{I}, \quad C_{\text{rs}}^2(\mathbf{y}) = \frac{1}{2} \mathbf{J} \cdot \mathbf{J}, \quad C_{\text{rs}}^3(\mathbf{y}) = \frac{1}{2} \mathbf{K} \cdot \mathbf{K}, \\ C_{\text{rs}}^4(\mathbf{y}) = \mathbf{J} \cdot \mathbf{K}, \quad C_{\text{rs}}^5(\mathbf{y}) = \mathbf{K} \cdot \mathbf{I}, \quad C_{\text{rs}}^6(\mathbf{y}) = \mathbf{I} \cdot \mathbf{J}. \quad (78)$$

Indeed, it can be checked that

$$\ker \mathbf{B}_{\text{rs}}(\mathbf{y}) = \text{span} \left\{ \begin{pmatrix} \mathbf{0} \\ \mathbf{I} \\ \mathbf{0} \\ \mathbf{0} \end{pmatrix}, \begin{pmatrix} \mathbf{0} \\ \mathbf{0} \\ \mathbf{J} \\ \mathbf{0} \end{pmatrix}, \begin{pmatrix} \mathbf{0} \\ \mathbf{0} \\ \mathbf{0} \\ \mathbf{K} \end{pmatrix}, \begin{pmatrix} \mathbf{0} \\ \mathbf{0} \\ \mathbf{K} \\ \mathbf{J} \end{pmatrix}, \begin{pmatrix} \mathbf{0} \\ \mathbf{K} \\ \mathbf{0} \\ \mathbf{I} \end{pmatrix}, \begin{pmatrix} \mathbf{0} \\ \mathbf{J} \\ \mathbf{I} \\ \mathbf{0} \end{pmatrix} \right\}. \quad (79)$$

Let  $F_{\text{rs}}(\mathbf{y}) = H_{\text{rs}}^0(\mathbf{y}) - \sum_i \mu_i C_{\text{rs}}^i(\mathbf{y})$ . The condition  $\nabla_{\mathbf{y}} F_{\text{rs}}(\mathbf{y}_e) = \mathbf{0}$  leads to

$$\mathbb{I}^{-1} \boldsymbol{\Pi}_e - \boldsymbol{\Omega} = \boldsymbol{\omega}_e = \mathbf{0}, \quad (80)$$

$$\frac{(\mathbf{I}_e \cdot \boldsymbol{\Pi}_e)}{A} \boldsymbol{\Pi}_e + 3A \mathbf{S}_0 \mathbf{I}_e - \mu_1 \mathbf{I}_e - \mu_5 \mathbf{K}_e - \mu_6 \mathbf{J}_e = \mathbf{0}, \quad (81)$$

$$\frac{(\mathbf{J}_e \cdot \boldsymbol{\Pi}_e)}{B} \boldsymbol{\Pi}_e + 3B \mathbf{S}_0 \mathbf{J}_e - \mu_2 \mathbf{J}_e - \mu_4 \mathbf{K}_e - \mu_6 \mathbf{I}_e = \mathbf{0}, \quad (82)$$

$$\frac{(\mathbf{K}_e \cdot \boldsymbol{\Pi}_e)}{C} \boldsymbol{\Pi}_e + 3C \mathbf{S}_0 \mathbf{K}_e - \mu_3 \mathbf{K}_e - \mu_4 \mathbf{J}_e - \mu_5 \mathbf{I}_e = \mathbf{0}, \quad (83)$$

whose a solution is

$$\begin{aligned} \boldsymbol{\omega}_e &= \mathbf{0}, & \boldsymbol{\Pi}_e &= C \boldsymbol{\Omega} \mathbf{k}, & \mathbf{I}_e &= \mathbf{i}, & \mathbf{J}_e &= \mathbf{j}, & \mathbf{K}_e &= \mathbf{k}, \\ \mu_1 &= 3A \sigma_{xx}^0, & \mu_2 &= 3B \sigma_{yy}^0, & \mu_3 &= 3C \sigma_{zz}^0 + C \Omega^2, & \mu_4 &= \mu_5 = \mu_6 = 0. \end{aligned} \quad (84)$$

The other solutions are equivalent to this one but with a permutation of the moments of inertia  $A, B, C$ . The matrix  $\mathbf{A}_{\text{rs}}(\mathbf{y}_e)$  of the linearised system is given by Eq. (40). To simplify the result, we perform the change of variables  $\delta \mathbf{y} = \mathbf{P} \delta \mathbf{y}^*$  with

$$\begin{aligned} \delta \mathbf{y}^* &= \left( \delta \Pi_z, \delta I_y, \delta \Pi_x, \delta \Pi_y, \delta I_z, \delta J_z, \delta I_x, \delta J_y, \delta K_z, \right. \\ &\quad \left. \delta I_y + \delta J_x, \delta I_z + \delta K_x, \delta J_z + \delta K_y \right)^{\text{T}}. \end{aligned} \quad (85)$$

The first two components of  $\delta \mathbf{y}^*$  are associated with the libration in longitude, the next four components describe the wobble and the libration in latitude, and finally, the last six coordinates being in the kernel of  $\mathbf{B}_{\text{rs}}(\mathbf{y}_e)$  remain identically equal to zero. Let  $\mathbf{A}_{\text{rs}}^*(\mathbf{y}_e)$  be the matrix of the linear system in the new variables  $\delta \mathbf{y}^*$ , i.e.,  $\mathbf{A}_{\text{rs}}^* = \mathbf{P}^{-1} \mathbf{A}_{\text{rs}} \mathbf{P}$ , and let  $\mathbf{A}_{\text{rs}}^1$  and  $\mathbf{A}_{\text{rs}}^2$  be the respective  $2 \times 2$  and  $4 \times 4$  matrices such that

$$\mathbf{A}_{\text{rs}}^*(\mathbf{y}_e) = \begin{bmatrix} \mathbf{A}_{\text{rs}}^1 & \mathbf{0} & \cdot \\ \mathbf{0} & \mathbf{A}_{\text{rs}}^2 & \cdot \\ \mathbf{0} & \mathbf{0} & \mathbf{0} \end{bmatrix} \quad (86)$$

where the dots  $\cdot$  represent arbitrary matrices not influencing the motion. We have

$$\mathbf{A}_{\text{rs}}^1 = \begin{bmatrix} 0 & -3(B-A)(\sigma_{xx}^0 - \sigma_{yy}^0) \\ 1/C & 0 \end{bmatrix}, \quad (87)$$

and

$$\mathbf{A}_{\text{rs}}^2 = \begin{bmatrix} 0 & \Omega & 0 & 3(C-B)(\sigma_{zz}^0 - \sigma_{yy}^0) \\ -\Omega & 0 & 3(C-A)(\sigma_{xx}^0 - \sigma_{zz}^0) & 0 \\ 0 & -\frac{1}{B} & 0 & -\frac{C-B}{B} \Omega \\ \frac{1}{A} & 0 & \frac{C-A}{A} \Omega & 0 \end{bmatrix}. \quad (88)$$

Hence, the frequency of libration in longitude  $\omega_{\text{rs},u}$ , which is the eigenvalue of  $\mathbf{A}_{\text{rs}}^1$ , reads

$$\omega_{\text{rs},u} = \sqrt{3\gamma(\kappa_1 - \kappa_2)}, \quad (89)$$

and the frequencies associated with the wobble  $\omega_{\text{rs},w}$  and the libration in latitude  $\omega_{\text{rs},v}$ , the eigenvalues of  $\mathbf{A}_{\text{rs}}^2$ , are given by

$$\omega_{\text{rs},w} = \left( \frac{p - \sqrt{p^2 - 4q}}{2} \right)^{1/2}, \quad \omega_{\text{rs},v} = \left( \frac{p + \sqrt{p^2 - 4q}}{2} \right)^{1/2} \quad (90)$$

with

$$p = (1 + \alpha\beta)\Omega^2 + 3(\beta\kappa_1 + \alpha\kappa_2), \quad (91)$$

$$q = \alpha\beta \left( \Omega^4 + 3(\kappa_1 + \kappa_2)\Omega^2 + 9\kappa_1\kappa_2 \right), \quad (92)$$

$$\kappa_1 = \sigma_{xx}^0 - \sigma_{zz}^0, \quad (93)$$

$$\kappa_2 = \sigma_{yy}^0 - \sigma_{zz}^0, \quad (94)$$

and

$$\alpha = \frac{C - B}{A}, \quad \beta = \frac{C - A}{B}, \quad \gamma = \frac{B - A}{C}. \quad (95)$$

Here we retrieve the well-known eigenfrequencies of a rigid satellite close to the synchronous equilibrium state (e.g., [Rambaux et al., 2012](#)). Let us nevertheless stress that Eqs. (89) and (90) are associated with the motion of the *three* vectors ( $\mathbf{I}, \mathbf{J}, \mathbf{K}$ ) in the rotating frame. By consequence, if we denote by  $\bar{\omega}_{\text{rs},v} \approx 3\beta\Omega/2$  the frequency of libration in latitude associated with the motion of the *sole* vector  $\mathbf{K}$  with respect to the inertial frame (as it is commonly defined for an axisymmetric body), we have  $\omega_{\text{rs},v} = \bar{\omega}_{\text{rs},v} + \Omega$ .

### 3.2 Stability

For this problem, the Lyapunov function  $N_{\text{rs}}(\mathbf{y})$ , as defined in Eq. (43), is

$$\begin{aligned} N_{\text{rs}}(\mathbf{y}) = & \frac{1}{2A} \left( \Pi_x + \frac{1}{2}(C - A)\Omega(I_z - K_x) \right)^2 + \frac{1}{2B} \left( \Pi_y + \frac{1}{2}(C - B)\Omega(J_z - K_y) \right)^2 \\ & + \frac{1}{2C} \Pi_z^2 + \frac{1}{2}n_1(I_y - J_x)^2 + \frac{1}{2}n_2(I_z - K_x)^2 + \frac{1}{2}n_3(J_z - K_y)^2 \end{aligned} \quad (96)$$

with

$$n_1 = \frac{3}{4}(B - A)(\kappa_1 - \kappa_2), \quad n_2 = \frac{1}{8}(C - A)(\Omega^2 + 3\kappa_1), \quad n_3 = \frac{1}{8}(C - B)(\Omega^2 + 3\kappa_2). \quad (97)$$

We recall that the system is nonlinearly stable if  $N_{\text{rs}}(\mathbf{y})$  is a strictly convex function. Coefficients  $A$ ,  $B$ , and  $C$  are positive, as required. The nonlinear stability is then achieved when  $n_1$ ,  $n_2$ , and  $n_3$  are all positive. Given that  $\kappa_1 > \kappa_2 > 0$  at low inclination  $i$ , the criterion implies  $C > B > A$ , which is the well-known stability condition for this classical equilibrium where the longest axis points towards the parent planet (e.g. [Beck and Hall, 1998](#)).



### 3.3 Driven solution

Here we look for the forced solution when the time-dependent perturbation  $H_{rs}^1(t)$  is taken into account. In the variables  $\delta\mathbf{y}^*$  (Eq. 85), and with the notation of Eq. (41), the perturbation  $\delta\mathbf{z}_{rs}^*(t)$  is given by

$$\delta\mathbf{z}_{rs}^*(t) = -\mathbf{P}^{-1}\mathbf{B}_{rs}(\mathbf{y}_e)\nabla_{\mathbf{y}}H_{rs}^1(\mathbf{y}_e, t). \quad (98)$$

To match the notation of the matrix  $\mathbf{A}_{rs}^*$ , let  $\delta\mathbf{y}^1$  and  $\delta\mathbf{y}^2$  be the first 2 and the next 4 components of  $\delta\mathbf{y}^*$ , idem for  $\delta\mathbf{z}_{rs}^*(t)$ , such that the linear problem with perturbation reads

$$\delta\dot{\mathbf{y}}^k - \mathbf{A}_{rs}^k\delta\mathbf{y}^k = \delta\mathbf{z}_{rs}^k(t), \quad k = 1, 2. \quad (99)$$

By definition,

$$\delta\mathbf{y}^1 = (\delta\Pi_z, \delta I_y)^\top, \quad \delta\mathbf{y}^2 = (\delta\Pi_x, \delta\Pi_y, \delta I_z, \delta J_z)^\top, \quad (100)$$

and Eq. (98) implies

$$\delta\mathbf{z}_{rs}^1(t) = \begin{pmatrix} 3(B-A)\sigma_{xy}^1(t) \\ 0 \end{pmatrix}, \quad \delta\mathbf{z}_{rs}^2(t) = \begin{pmatrix} 3(C-B)\sigma_{yz}^1(t) \\ -3(C-A)\sigma_{xz}^1(t) \\ 0 \\ 0 \end{pmatrix}. \quad (101)$$

Note that the term  $\sigma_{yz}^1(t)$  is present in the perturbation  $\delta\mathbf{z}_{rs}^2(t)$  but its effect on the orientation of the spin axis is very weak. For instance, according to the ephemeris of Titan in TASS1.6 (Vienne and Duriez, 1995), the amplitude associated with the angle  $(\Omega t - \Phi)$  in  $\sigma_{yz}^1(t)$  is about 500 times lower than that in  $\sigma_{xz}^1(t)$ . In the numerical applications (Sect. 6),  $\sigma_{yz}^1(t)$  is simply discarded.

## 4 Satellite with a liquid core

In this section we consider a satellite with a rigid mantle/crust layer surrounding a liquid core. In a first step, we analyse the problem using the Poincaré-Hough model which is valid for all eccentricities of the ellipsoidal cavity containing the fluid core (Poincaré, 1910; Hough, 1895). In a second one, we truncate the problem at the first order with respect to the equatorial and polar flattening of the cavity. The same simplification will be used again in Sect. 5 where the case of a satellite with a subsurface ocean is treated. Here, the two models of the same problem are used to estimate the error made by the approximation.

### 4.1 Poincaré-Hough model

As in the previous model,  $A, B, C$  designate the principal moments of inertia of the whole satellite. Those of the liquid core are denote by  $A_c, B_c, C_c$ . We assume that the axes of the core/mantle ellipsoidal boundary are aligned to those of the satellite surface. Hence, the principal axes  $(\mathbf{I}_c, \mathbf{J}_c, \mathbf{K}_c)$  of the core are aligned to those of the mantle denoted  $(\mathbf{I}_m, \mathbf{J}_m, \mathbf{K}_m)$  which are also aligned to those of the whole satellite

( $\mathbf{I}, \mathbf{J}, \mathbf{K}$ ). The vector  $\boldsymbol{\omega}$  still represents the rotation vector of ( $\mathbf{I}, \mathbf{J}, \mathbf{K}$ ) with respect to the laboratory frame expressed in the laboratory frame. We add the rotation vector  $\boldsymbol{\omega}'_c$  associated with the *simple motion* of the liquid core with respect to the mantle and expressed in the mantle-fixed frame (Poincaré, 1910). As in the rigid case, the laboratory frame rotates with respect to the inertial frame at the speed  $\boldsymbol{\Omega}$ . Let  $\mathbb{I}$ ,  $\mathbb{I}'_c$  and  $\mathbb{I}'$  be the inertia matrices defined as

$$\mathbb{I} = \mathbf{R} \text{diag}(A, B, C) \mathbf{R}^T, \quad (102)$$

$$\mathbb{I}'_c = \text{diag}(A_c, B_c, C_c), \quad (103)$$

$$\mathbb{I}' = \text{diag}(A', B', C') \mathbf{R}^T, \quad (104)$$

where  $\mathbf{R} = [\mathbf{I}, \mathbf{J}, \mathbf{K}]$  is the rotation matrix of the mantle relative to the laboratory frame. Furthermore, we have defined

$$A' = A_c \sqrt{1 - \alpha_c^2}, \quad B' = B_c \sqrt{1 - \beta_c^2}, \quad C' = C_c \sqrt{1 - \gamma_c^2}, \quad (105)$$

with

$$\alpha_c = \frac{C_c - B_c}{A_c}, \quad \beta_c = \frac{C_c - A_c}{B_c}, \quad \gamma_c = \frac{B_c - A_c}{C_c}. \quad (106)$$

For this problem, the Lie velocity is  $\boldsymbol{\eta} = (\boldsymbol{\omega}, \boldsymbol{\omega}'_c)$  and the generalised coordinates are limited to  $\mathbf{q} = (\mathbf{I}, \mathbf{J}, \mathbf{K})$ . Coordinates associated with the simple motion of the liquid core do not appear in the equations of motion because the fluid is assumed to be incompressible and its volume is set by the mantle, thus the kinetic and the potential energies only depends on  $\boldsymbol{\eta}$  and  $\mathbf{q}$ . The kinetic energy  $T_{fc}(\boldsymbol{\eta}, \mathbf{q})$  of rotation of the satellite is (Poincaré, 1910; Hough, 1895)

$$T_{fc}(\boldsymbol{\eta}, \mathbf{q}) = \frac{(\boldsymbol{\omega} + \boldsymbol{\Omega})^T \mathbb{I} (\boldsymbol{\omega} + \boldsymbol{\Omega})}{2} + \frac{\boldsymbol{\omega}'_c{}^T \mathbb{I}'_c \boldsymbol{\omega}'_c}{2} + \boldsymbol{\omega}'_c{}^T \mathbb{I}' (\boldsymbol{\omega} + \boldsymbol{\Omega}), \quad (107)$$

The potential energy is the same as in the rigid satellite case (see sect. 3). Thus, the Lagrangian  $L_{fc}(\boldsymbol{\eta}, \mathbf{q})$  reads

$$L_{fc}(\boldsymbol{\eta}, \mathbf{q}) = \frac{(\boldsymbol{\omega} + \boldsymbol{\Omega})^T \mathbb{I} (\boldsymbol{\omega} + \boldsymbol{\Omega})}{2} + \frac{\boldsymbol{\omega}'_c{}^T \mathbb{I}'_c \boldsymbol{\omega}'_c}{2} + \boldsymbol{\omega}'_c{}^T \mathbb{I}' (\boldsymbol{\omega} + \boldsymbol{\Omega}) - \frac{3\mathcal{G}M_p}{2} \frac{\mathbf{r}^T \mathbb{I} \mathbf{r}}{r^5}. \quad (108)$$

The Lie momenta associated with  $\boldsymbol{\omega}$  and  $\boldsymbol{\omega}'_c$  are respectively

$$\boldsymbol{\Pi} = \frac{\partial L_{fc}}{\partial \boldsymbol{\omega}} = \mathbb{I} (\boldsymbol{\omega} + \boldsymbol{\Omega}) + \mathbb{I}'^T \boldsymbol{\omega}'_c, \quad (109)$$

$$\boldsymbol{\Pi}'_c = \frac{\partial L_{fc}}{\partial \boldsymbol{\omega}'_c} = \mathbb{I}'_c \boldsymbol{\omega}'_c + \mathbb{I}' (\boldsymbol{\omega} + \boldsymbol{\Omega}), \quad (110)$$

with the inverse transformation,

$$\boldsymbol{\omega} = \mathbb{Q} \boldsymbol{\Pi} - \mathbb{Q}'^T \boldsymbol{\Pi}'_c - \boldsymbol{\Omega}, \quad (111)$$

$$\boldsymbol{\omega}'_c = \mathbb{Q}'_c \boldsymbol{\Pi}'_c - \mathbb{Q}' \boldsymbol{\Pi}, \quad (112)$$

where

$$\mathbb{Q} = \mathbf{R} \text{diag} \left( \frac{A_c}{AA_c - A'^2}, \frac{B_c}{BB_c - B'^2}, \frac{C_c}{CC_c - C'^2} \right) \mathbf{R}^T, \quad (113)$$

$$\mathbb{Q}'_c = \text{diag} \left( \frac{A}{AA_c - A'^2}, \frac{B}{BB_c - B'^2}, \frac{C}{CC_c - C'^2} \right), \quad (114)$$

$$\mathbb{Q}' = \text{diag} \left( \frac{A'}{AA_c - A'^2}, \frac{B'}{BB_c - B'^2}, \frac{C'}{CC_c - C'^2} \right) \mathbf{R}^T. \quad (115)$$

The Hamiltonian of the problem is then

$$H_{\text{fc}}(\mathbf{y}, t) = \frac{\boldsymbol{\Pi}^T \mathbf{Q} \boldsymbol{\Pi}}{2} + \frac{\boldsymbol{\Pi}'^T \mathbf{Q}' \boldsymbol{\Pi}'_c}{2} - \boldsymbol{\Pi}'^T \mathbf{Q}' \boldsymbol{\Pi} - \boldsymbol{\Omega}^T \boldsymbol{\Pi} + \frac{3\mathcal{G}M_p}{2} \frac{\mathbf{r}^T \mathbb{I} \mathbf{r}}{r^5}, \quad (116)$$

with the state vector  $\mathbf{y} = (\boldsymbol{\Pi}'_c, \boldsymbol{\Pi}, \mathbf{I}, \mathbf{J}, \mathbf{K})$ . In these variables, the Poisson matrix reads

$$\mathbf{B}_{\text{fc}}(\mathbf{y}) = \begin{bmatrix} \hat{\boldsymbol{\Pi}}'_c & \mathbf{0} & \mathbf{0} & \mathbf{0} & \mathbf{0} \\ \mathbf{0} & \hat{\boldsymbol{\Pi}} & \hat{\mathbf{I}} & \hat{\mathbf{J}} & \hat{\mathbf{K}} \\ \mathbf{0} & \hat{\mathbf{I}} & \mathbf{0} & \mathbf{0} & \mathbf{0} \\ \mathbf{0} & \hat{\mathbf{J}} & \mathbf{0} & \mathbf{0} & \mathbf{0} \\ \mathbf{0} & \hat{\mathbf{K}} & \mathbf{0} & \mathbf{0} & \mathbf{0} \end{bmatrix} \quad (117)$$

and the equations of motion are

$$\dot{\boldsymbol{\Pi}}'_c = \boldsymbol{\omega}'_c \times \boldsymbol{\Pi}'_c, \quad (118)$$

$$\dot{\boldsymbol{\Pi}} = \boldsymbol{\Pi} \times \boldsymbol{\Omega} - 3 \frac{\mathcal{G}M_p}{r^5} (\mathbb{I} \mathbf{r}) \times \mathbf{r}, \quad (119)$$

$$\dot{\mathbf{I}} = \boldsymbol{\omega} \times \mathbf{I}, \quad (120)$$

$$\dot{\mathbf{J}} = \boldsymbol{\omega} \times \mathbf{J}, \quad (121)$$

$$\dot{\mathbf{K}} = \boldsymbol{\omega} \times \mathbf{K}. \quad (122)$$

As in the rigid case (Sect. 3), we now split the Hamiltonian  $H_{\text{fc}}(\mathbf{y}, t)$  into its autonomous part  $H_{\text{fc}}^0(\mathbf{y})$  and a perturbation  $H_{\text{fc}}^1(\mathbf{y}, t)$  using the decomposition of the gravitational potential energy  $U_0(\mathbf{y})$  and  $U_1(\mathbf{y}, t)$ , Eqs. (61-62). There are seven Casimir functions given by

$$\begin{aligned} C_{\text{fc}}^0(\mathbf{y}) &= \frac{1}{2} \boldsymbol{\Pi}'_c \cdot \boldsymbol{\Pi}'_c, \\ C_{\text{fc}}^1(\mathbf{y}) &= \frac{1}{2} \mathbf{I} \cdot \mathbf{I}, \quad C_{\text{fc}}^2(\mathbf{y}) = \frac{1}{2} \mathbf{J} \cdot \mathbf{J}, \quad C_{\text{fc}}^3(\mathbf{y}) = \frac{1}{2} \mathbf{K} \cdot \mathbf{K}, \\ C_{\text{fc}}^4(\mathbf{y}) &= \mathbf{J} \cdot \mathbf{K}, \quad C_{\text{fc}}^5(\mathbf{y}) = \mathbf{K} \cdot \mathbf{I}, \quad C_{\text{fc}}^6(\mathbf{y}) = \mathbf{I} \cdot \mathbf{J}. \end{aligned} \quad (123)$$

The equilibrium  $\mathbf{y}_e$  of  $H_{\text{fc}}^0(\mathbf{y})$  is solution of

$$\boldsymbol{\omega}'_{c,e} - \mu_0 \boldsymbol{\Pi}'_{c,e} = \mathbf{0}, \quad (124)$$

$$\boldsymbol{\omega}_e = \mathbf{0}, \quad (125)$$

$$\frac{A_c(\mathbf{I}_e \cdot \boldsymbol{\Pi}_e) - A'(\mathbf{I}_e \cdot \boldsymbol{\Pi}'_{c,e})}{AA_c - A'^2} \boldsymbol{\Pi}_e + 3A\mathbf{S}_0 \mathbf{I}_e - \mu_1 \mathbf{I}_e - \mu_5 \mathbf{K}_e - \mu_6 \mathbf{J}_e = \mathbf{0}, \quad (126)$$

$$\frac{B_c(\mathbf{J}_e \cdot \boldsymbol{\Pi}_e) - B'(\mathbf{J}_e \cdot \boldsymbol{\Pi}'_{c,e})}{BB_c - B'^2} \boldsymbol{\Pi}_e + 3B\mathbf{S}_0 \mathbf{J}_e - \mu_2 \mathbf{J}_e - \mu_4 \mathbf{K}_e - \mu_6 \mathbf{I}_e = \mathbf{0}, \quad (127)$$

$$\frac{C_c(\mathbf{K}_e \cdot \boldsymbol{\Pi}_e) - C'(\mathbf{K}_e \cdot \boldsymbol{\Pi}'_{c,e})}{CC_c - C'^2} \boldsymbol{\Pi}_e + 3C\mathbf{S}_0 \mathbf{K}_e - \mu_3 \mathbf{K}_e - \mu_4 \mathbf{J}_e - \mu_5 \mathbf{I}_e = \mathbf{0}. \quad (128)$$

We stress that  $\boldsymbol{\Pi}$  is written in the laboratory frame while  $\boldsymbol{\Pi}'_c$  is expressed in the mantle-fixed frame. Thus, in Eq. (126),  $(\mathbf{I} \cdot \boldsymbol{\Pi}) = I_x \Pi_x + I_y \Pi_y + I_z \Pi_z$  whereas  $(\mathbf{I} \cdot \boldsymbol{\Pi}'_c) = I'_{c,x} \Pi'_c$ . The same reasoning holds in Eqs. (127,128). The norm of the angular velocity  $\boldsymbol{\omega}'_{c,e}$  can be arbitrarily chosen. This is due to the conservation of the Casimir  $C_{\text{fc}}^0(\mathbf{y})$ . Here, we assume that the fluid core has no mean angular

velocity with respect to the mantle and thus  $\boldsymbol{\omega}'_{c,e} = \mathbf{0}$ . Under this hypothesis, we get

$$\begin{aligned} \boldsymbol{\omega}_e &= \mathbf{0}, \quad \boldsymbol{\Pi}'_{c,e} = C'\Omega\mathbf{k}, \quad \boldsymbol{\Pi}_e = C\Omega\mathbf{k}, \quad \mathbf{I}_e = \mathbf{i}, \quad \mathbf{J}_e = \mathbf{j}, \quad \mathbf{K}_e = \mathbf{k}, \\ \mu_0 &= 0, \quad \mu_1 = 3A\sigma_{xx}^0, \quad \mu_2 = 3B\sigma_{yy}^0, \quad \mu_3 = 3C\sigma_{zz}^0 + C\Omega^2, \quad \mu_4 = \mu_5 = \mu_6 = 0. \end{aligned} \quad (129)$$

The linear system is expressed in the coordinates

$$\begin{aligned} \delta\mathbf{y}^* &= \left( \delta\Pi_z, \delta I_y, \delta\Pi'_{c,x}, \delta\Pi'_{c,y}, \delta\Pi_x, \delta\Pi_y, \delta I_z, \delta J_z, \delta\Pi'_{c,z}, \delta I_x, \delta J_y, \delta K_z, \right. \\ &\quad \left. \delta I_y + \delta J_x, \delta I_z + \delta K_x, \delta J_z + \delta K_y \right)^T. \end{aligned} \quad (130)$$

Let  $\mathbf{A}_{fc}^*(\mathbf{y}_e)$  be the matrix of the linear system evaluated at the equilibrium point and expressed in the coordinates  $\delta\mathbf{y}^*$ . As in the rigid case, we define the matrices  $\mathbf{A}_{fc}^1$  and  $\mathbf{A}_{fc}^2$  such that

$$\mathbf{A}_{fc}^*(\mathbf{y}_e) = \begin{bmatrix} \mathbf{A}_{fc}^1 & \mathbf{0} & \cdot \\ \mathbf{0} & \mathbf{A}_{fc}^2 & \cdot \\ \mathbf{0} & \mathbf{0} & \mathbf{0} \end{bmatrix}, \quad (131)$$

where the dots  $\cdot$  still denote arbitrary matrices. We get

$$\mathbf{A}_{fc}^1 = \begin{bmatrix} 0 & -3(B-A)(\sigma_{xx}^0 - \sigma_{yy}^0) \\ C_c & 0 \\ CC_c - C'^2 & 0 \end{bmatrix}, \quad (132)$$

and

$$\mathbf{A}_{fc}^2 = \begin{bmatrix} 0 & \frac{C'}{\underline{B}}\Omega & 0 & -\frac{C'}{\underline{B}'}\Omega & 0 & -\frac{C'}{\underline{B}'}C\Omega^2 \\ -\frac{C'}{\underline{A}}\Omega & 0 & \frac{C'}{\underline{A}'}\Omega & 0 & \frac{C'}{\underline{A}'}C\Omega^2 & 0 \\ 0 & 0 & 0 & \Omega & 0 & -3(C-B)\kappa_2 \\ 0 & 0 & -\Omega & 0 & 3(C-A)\kappa_1 & 0 \\ 0 & \frac{1}{\underline{B}'} & 0 & -\frac{1}{\underline{B}_c} & 0 & \left(1 - \frac{C}{\underline{B}_c}\right)\Omega \\ -\frac{1}{\underline{A}'} & 0 & \frac{1}{\underline{A}_c} & 0 & -\left(1 - \frac{C}{\underline{A}_c}\right)\Omega & 0 \end{bmatrix} \quad (133)$$

with

$$\begin{aligned} \frac{1}{\underline{A}} &= \frac{A}{AA_c - A'^2}, & \frac{1}{\underline{A}_c} &= \frac{A_c}{AA_c - A'^2}, & \frac{1}{\underline{A}'} &= \frac{A'}{AA_c - A'^2}, \\ \frac{1}{\underline{B}} &= \frac{B}{BB_c - B'^2}, & \frac{1}{\underline{B}_c} &= \frac{B_c}{BB_c - B'^2}, & \frac{1}{\underline{B}'} &= \frac{B'}{BB_c - B'^2}, \\ \frac{1}{\underline{C}} &= \frac{C}{CC_c - C'^2}, & \frac{1}{\underline{C}_c} &= \frac{C_c}{CC_c - C'^2}, & \frac{1}{\underline{C}'} &= \frac{C'}{CC_c - C'^2}. \end{aligned} \quad (134)$$

The eigenfrequencies are

$$\omega_{\text{fc},u} = \left( \frac{CC_c}{CC_c - C'^2} \right)^{1/2} \omega_{\text{rs},u}, \quad (135)$$

$$\omega_{\text{fc},v} = \omega_{\text{rs},v} + O(\epsilon), \quad (136)$$

$$\omega_{\text{fc},w} = \omega_{\text{rs},w} + O(\epsilon), \quad (137)$$

$$\omega_{\text{fc},z} = \frac{C'}{\sqrt{A_c B_c}} \Omega + O(\epsilon) \quad (138)$$

with  $\epsilon$  being the mass of the core divided by the total mass of the satellite.  $\omega_{\text{rs},u}$ ,  $\omega_{\text{rs},v}$ , and  $\omega_{\text{rs},w}$  are the frequencies obtained in the rigid case (Eqs. 89,90).  $\omega_{\text{fc},z}$  is the frequency of the additional degree of freedom induced by the presence of the liquid core. In the case where the fluid core represents a significant fraction of the total mass of the satellite, Eqs. (136-138) are no longer valid and eigenfrequencies should be directly computed from the matrix  $\mathbf{A}_{\text{fc}}^2$  (Eq. 133).

The Lyapunov function (Eq. 43) associated with this problem is

$$\begin{aligned} N_{\text{fc}}(\mathbf{y}) = & \frac{1}{2\underline{A}_c} \left( \Pi_x - \frac{A'}{A_c} \Pi'_{c,x} + \frac{1}{2} (C - \underline{A}_c) (I_z - K_x) \right)^2 \\ & + \frac{1}{2\underline{B}_c} \left( \Pi_y - \frac{B'}{B_c} \Pi'_{c,y} + \frac{1}{2} (C - \underline{B}_c) (J_z - K_y) \right)^2 + \frac{1}{2\underline{C}_c} \Pi_z^2 \\ & + \frac{1}{2A_c} \left( \Pi'_{c,x} - \frac{1}{2} A' \Omega (I_z - K_x) \right)^2 + \frac{1}{2B_c} \left( \Pi'_{c,y} - \frac{1}{2} B' \Omega (J_z - K_y) \right)^2 \\ & + \frac{1}{2} n_1 (I_y - J_x)^2 + \frac{1}{2} n_2 (I_z - K_x)^2 + \frac{1}{2} n_3 (J_z - K_y)^2, \end{aligned} \quad (139)$$

where  $n_1$ ,  $n_2$ , and  $n_3$  are the same as in the rigid case (see Eq. 97). Given that  $\underline{A}_c$ ,  $\underline{B}_c$ ,  $\underline{C}_c$ ,  $A_c$ , and  $B_c$  are all positive, the nonlinear stability criterion is identical to that of a rigid satellite, namely  $C > B > A$ . In particular, there is no restriction on the moments of inertia of the core ( $A_c, B_c, C_c$ ).

The driven equations of motion of the satellite with a liquid core in the vicinity of the relative equilibrium  $\mathbf{y}_e$  are of the form

$$\delta \dot{\mathbf{y}}^k - \mathbf{A}_{\text{fc}}^k \delta \mathbf{y}^k = \delta \mathbf{z}_{\text{fc}}^k(t), \quad k = 1, 2, \quad (140)$$

with

$$\delta \mathbf{y}^1 = (\delta \Pi_z, \delta I_y)^\top, \quad \delta \mathbf{y}^2 = (\delta \Pi'_{c,x}, \delta \Pi'_{c,y}, \delta \Pi_x, \delta \Pi_y, \delta I_z, \delta J_z)^\top, \quad (141)$$

and

$$\delta \mathbf{z}_{\text{fc}}^1(t) = \begin{pmatrix} 3(B - A) \sigma_{xy}^1(t) \\ 0 \end{pmatrix}, \quad \delta \mathbf{z}_{\text{fc}}^2(t) = \begin{pmatrix} 3(C - B) \sigma_{yz}^1(t) \\ -3(C - A) \sigma_{xz}^1(t) \\ 0 \\ 0 \\ 0 \\ 0 \end{pmatrix}. \quad (142)$$

## 4.2 Quasi-spherical approximation

In this section, we reconsider the case of a satellite with a liquid core, but we assimilate  $A'$ ,  $B'$  and  $C'$  to the moments of inertia of the core, i.e., we assume

$$A' \approx A_c, \quad B' \approx B_c, \quad C' \approx C_c. \quad (143)$$

According to Eq. (105), this is equivalent to a first order approximation in  $\alpha_c$ ,  $\beta_c$  and  $\gamma_c$ . With this simplification, the kinetic energy (Eq. 107) can be rewritten as follows

$$T_{\text{fc}'}(\boldsymbol{\eta}, \mathbf{q}) = \frac{(\boldsymbol{\omega} + \boldsymbol{\Omega})^T \mathbb{I}_m (\boldsymbol{\omega} + \boldsymbol{\Omega})}{2} + \frac{(\boldsymbol{\omega}'_c + \mathbf{R}^T (\boldsymbol{\omega} + \boldsymbol{\Omega}))^T \mathbb{I}'_c (\boldsymbol{\omega}'_c + \mathbf{R}^T (\boldsymbol{\omega} + \boldsymbol{\Omega}))}{2} \quad (144)$$

where

$$\begin{aligned} \mathbb{I}_m &= \mathbb{I} - \mathbf{R} \mathbb{I}'_c \mathbf{R}^T \\ &= \mathbf{R} \text{diag}(A_m, B_m, C_m) \mathbf{R}^T \end{aligned} \quad (145)$$

is the inertia tensor of the mantle written in the laboratory frame ( $A_m = A - A_c$ ,  $B_m = B - B_c$ , and  $C_m = C - C_c$ ). According to the expression (144), the problem behaves as if the liquid core were rotating rigidly relative to the mantle at the angular velocity  $\boldsymbol{\omega}'_c$  with a matrix of inertia  $\mathbb{I}'_c$  constant in the mantle-fixed frame. Indeed,  $\boldsymbol{\omega}'_c + \mathbf{R}^T (\boldsymbol{\omega} + \boldsymbol{\Omega})$  is the rotation speed of the core with respect to the inertial frame written in the mantle-fixed frame. We here retrieve the approximation made by Mathews et al. (1991) who neglected the small departure of the fluid velocity field from a pure solid rotation. Following the same procedure as in Sect. 4.1, the two submatrices of the linearised system written in the set of variables  $\delta \mathbf{y}^*$  (Eq. 130) become

$$\mathbf{A}_{\text{fc}'}^1 = \begin{bmatrix} 0 & -3(B - A)(\sigma_{xx}^0 - \sigma_{yy}^0) \\ \frac{1}{C_m} & 0 \end{bmatrix}, \quad (146)$$

and

$$\mathbf{A}_{\text{fc}'}^2 = \begin{bmatrix} 0 & \frac{BC_c}{B_m B_c} \Omega & 0 & -\frac{C_c}{B_m} \Omega & 0 & -\frac{CC_c}{B_m} \Omega^2 \\ -\frac{AC_c}{A_m A_c} \Omega & 0 & -\frac{C_c}{A_m} \Omega & 0 & \frac{CC_c}{A_m} \Omega^2 & 0 \\ 0 & 0 & 0 & \Omega & 0 & -3(C - B)\kappa_2 \\ 0 & 0 & -\Omega & 0 & 3(C - A)\kappa_1 & 0 \\ 0 & \frac{1}{B_m} & 0 & -\frac{1}{B_m} & 0 & \left(1 - \frac{C}{B_m}\right) \Omega \\ -\frac{1}{A_m} & 0 & \frac{1}{A_m} & 0 & -\left(1 - \frac{C}{A_m}\right) \Omega & 0 \end{bmatrix}. \quad (147)$$

Although we retrieve the eigenfrequencies obtained in section 4.1 within the approximation (Eq. 143) only, the second member  $\delta \mathbf{z}_{\text{fc}'}(t)$  of the driven system is exactly the same as  $\delta \mathbf{z}_{\text{fc}}(t)$  (Eq. 142).

## 5 Satellite with a subsurface ocean

Here, we consider a satellite with a rigid central part  $c$  (also called interior) and a rigid shell  $s$  separated by a global ocean  $o$ . By assumption, the shell is ellipsoidal with inner radii  $a_o, b_o, c_o$  and outer radii  $a_s, b_s, c_s$ . The interior, an ellipsoid of radii  $a_c, b_c, c_c$ , might be differentiated, i.e., it can be made of a succession of  $N$  concentric ellipsoidal layers with different densities  $(\rho_i)_{1 \leq i \leq N}$  and outer radii  $a_i, b_i, c_i$ . We have thus  $a_N = a_c, b_N = b_c$  and  $c_N = c_c$ . The ocean and the shell are assumed to be homogeneous with respective density  $\rho_o$  and  $\rho_s$ . Nevertheless, the results can easily be extended to the case of a stratified rigid shell. Because the simple motion introduced by Poincaré (1910) for a satellite with a liquid core cannot be applied in this case, we use the approximation described in Sect. 4.2. We could describe the evolution of the central region and of the ocean in the shell-fixed frame to remain close to the study made on the satellite with a liquid core, but equations are more symmetrical if all coordinates are given with respect to a same given frame which we chose to be the laboratory frame. In this frame, the configuration of the system is given by the coordinates of the principal axes of the interior and the shell, i.e., the generalised coordinates are  $\mathbf{q} = (\mathbf{I}_c, \mathbf{J}_c, \mathbf{K}_c, \mathbf{I}_s, \mathbf{J}_s, \mathbf{K}_s)$ . The Lie velocities are the rotation vectors of the three layers with respect to the laboratory frame  $\boldsymbol{\eta} = (\boldsymbol{\omega}_o, \boldsymbol{\omega}_c, \boldsymbol{\omega}_s)$ . Within the approximation of Sect. 4.2, the kinetic energy of the satellite with a global ocean reads

$$T_{\text{go}}(\boldsymbol{\eta}, \mathbf{q}) = \frac{(\boldsymbol{\omega}_c + \boldsymbol{\Omega})^T \mathbb{I}_c (\boldsymbol{\omega}_c + \boldsymbol{\Omega})}{2} + \frac{(\boldsymbol{\omega}_s + \boldsymbol{\Omega})^T \mathbb{I}_s (\boldsymbol{\omega}_s + \boldsymbol{\Omega})}{2} + \frac{(\boldsymbol{\omega}_o + \boldsymbol{\Omega})^T \mathbb{I}_o (\boldsymbol{\omega}_o + \boldsymbol{\Omega})}{2}, \quad (148)$$

with the inertia tensors

$$\mathbb{I}_c = \mathbf{R}_c \text{diag}(A_c, B_c, C_c) \mathbf{R}_c^T, \quad (149)$$

$$\mathbb{I}_s = \mathbf{R}_s \text{diag}(A_s, B_s, C_s) \mathbf{R}_s^T, \quad (150)$$

$$\mathbb{I}_o = \mathbf{R}_s \text{diag}(A'_s, B'_s, C'_s) \mathbf{R}_s^T - \mathbf{R}_c \text{diag}(A'_c, B'_c, C'_c) \mathbf{R}_c^T, \quad (151)$$

where  $\mathbf{R}_c = [\mathbf{I}_c, \mathbf{J}_c, \mathbf{K}_c]$ ,  $\mathbf{R}_s = [\mathbf{I}_s, \mathbf{J}_s, \mathbf{K}_s]$ , and

$$A_c = \sum_{i=1}^N \frac{4\pi}{15} \rho_i \left( a_i b_i c_i (b_i^2 + c_i^2) - a_{i-1} b_{i-1} c_{i-1} (b_{i-1}^2 + c_{i-1}^2) \right), \quad (152)$$

$$A_s = \frac{4\pi}{15} \rho_s \left( a_s b_s c_s (b_s^2 + c_s^2) - a_o b_o c_o (b_o^2 + c_o^2) \right), \quad (153)$$

$$A'_c = \frac{4\pi}{15} \rho_o a_c b_c c_c (b_c^2 + c_c^2), \quad (154)$$

$$A'_s = \frac{4\pi}{15} \rho_o a_o b_o c_o (b_o^2 + c_o^2). \quad (155)$$

In Eq. (152), we apply the convention  $a_0 = b_0 = c_0 = 0$ . The other quantities  $B, C$  are deduced from Eqs. (152-155) by circular permutation of  $a, b, c$ . Let us stress that the matrix of inertia of the whole satellite is simply

$$\mathbb{I} = \mathbb{I}_c + \mathbb{I}_s + \mathbb{I}_o. \quad (156)$$

In addition to the gravitational potential energy  $U(\mathbf{y}, t)$  between the planet point mass and the extended satellite, to get the Lagrangian we also need to include the self gravitational potential energy  $U_{\text{self}}(\mathbf{q})$  of the satellite as it is a function of the relative orientation of the interior and the shell. This potential energy reads (Laplace, 1798)

$$\begin{aligned} U_{\text{self}}(\mathbf{q}) &= \frac{u_{xx}}{2}(\mathbf{I}_c \cdot \mathbf{I}_s)^2 + \frac{u_{xy}}{2}(\mathbf{I}_c \cdot \mathbf{J}_s)^2 + \frac{u_{xz}}{2}(\mathbf{I}_c \cdot \mathbf{K}_s)^2 \\ &+ \frac{u_{yx}}{2}(\mathbf{J}_c \cdot \mathbf{I}_s)^2 + \frac{u_{yy}}{2}(\mathbf{J}_c \cdot \mathbf{J}_s)^2 + \frac{u_{yz}}{2}(\mathbf{J}_c \cdot \mathbf{K}_s)^2 \\ &+ \frac{u_{zx}}{2}(\mathbf{K}_c \cdot \mathbf{I}_s)^2 + \frac{u_{zy}}{2}(\mathbf{K}_c \cdot \mathbf{J}_s)^2 + \frac{u_{zz}}{2}(\mathbf{K}_c \cdot \mathbf{K}_s)^2, \end{aligned} \quad (157)$$

with

$$u_{xx} = \frac{8\pi}{15} \mathcal{G} (\rho_s f_s + (\rho_o - \rho_s) f_o) \sum_{i=1}^N (\rho_i - \rho_{i+1}) a_i^3 b_i c_i, \quad (158)$$

$$u_{xy} = \frac{8\pi}{15} \mathcal{G} (\rho_s g_s + (\rho_o - \rho_s) g_o) \sum_{i=1}^N (\rho_i - \rho_{i+1}) a_i^3 b_i c_i, \quad (159)$$

$$u_{xz} = \frac{8\pi}{15} \mathcal{G} (\rho_s h_s + (\rho_o - \rho_s) h_o) \sum_{i=1}^N (\rho_i - \rho_{i+1}) a_i^3 b_i c_i, \quad (160)$$

$$u_{yx} = \frac{8\pi}{15} \mathcal{G} (\rho_s f_s + (\rho_o - \rho_s) f_o) \sum_{i=1}^N (\rho_i - \rho_{i+1}) a_i b_i^3 c_i, \quad (161)$$

$$u_{yy} = \frac{8\pi}{15} \mathcal{G} (\rho_s g_s + (\rho_o - \rho_s) g_o) \sum_{i=1}^N (\rho_i - \rho_{i+1}) a_i b_i^3 c_i, \quad (162)$$

$$u_{yz} = \frac{8\pi}{15} \mathcal{G} (\rho_s h_s + (\rho_o - \rho_s) h_o) \sum_{i=1}^N (\rho_i - \rho_{i+1}) a_i b_i^3 c_i, \quad (163)$$

$$u_{zx} = \frac{8\pi}{15} \mathcal{G} (\rho_s f_s + (\rho_o - \rho_s) f_o) \sum_{i=1}^N (\rho_i - \rho_{i+1}) a_i b_i c_i^3, \quad (164)$$

$$u_{zy} = \frac{8\pi}{15} \mathcal{G} (\rho_s g_s + (\rho_o - \rho_s) g_o) \sum_{i=1}^N (\rho_i - \rho_{i+1}) a_i b_i c_i^3, \quad (165)$$

$$u_{zz} = \frac{8\pi}{15} \mathcal{G} (\rho_s h_s + (\rho_o - \rho_s) h_o) \sum_{i=1}^N (\rho_i - \rho_{i+1}) a_i b_i c_i^3, \quad (166)$$

where  $\rho_{N+1} := \rho_o$  and for  $* \in \{s, o\}$ ,

$$f_* = 2\pi \frac{a_* b_*}{c_*^2} \int_0^1 \left(1 + \frac{a_*^2 - c_*^2}{c_*^2} t^2\right)^{-3/2} \left(1 + \frac{b_*^2 - c_*^2}{c_*^2} t^2\right)^{-1/2} t^2 dt, \quad (167)$$

$$g_* = 2\pi \frac{a_* b_*}{c_*^2} \int_0^1 \left(1 + \frac{a_*^2 - c_*^2}{c_*^2} t^2\right)^{-1/2} \left(1 + \frac{b_*^2 - c_*^2}{c_*^2} t^2\right)^{-3/2} t^2 dt, \quad (168)$$

$$h_* = 2\pi \frac{a_* b_*}{c_*^2} \int_0^1 \left(1 + \frac{a_*^2 - c_*^2}{c_*^2} t^2\right)^{-1/2} \left(1 + \frac{b_*^2 - c_*^2}{c_*^2} t^2\right)^{-1/2} t^2 dt. \quad (169)$$

The Lagrangian  $L_{\text{go}}(\boldsymbol{\eta}, \mathbf{q})$  of the problem is then

$$\begin{aligned} L_{\text{go}}(\boldsymbol{\eta}, \mathbf{q}) &= \frac{(\boldsymbol{\omega}_c + \boldsymbol{\Omega})^\top \mathbb{I}_c (\boldsymbol{\omega}_c + \boldsymbol{\Omega})}{2} + \frac{(\boldsymbol{\omega}_s + \boldsymbol{\Omega})^\top \mathbb{I}_s (\boldsymbol{\omega}_s + \boldsymbol{\Omega})}{2} \\ &+ \frac{(\boldsymbol{\omega}_o + \boldsymbol{\Omega})^\top \mathbb{I}_o (\boldsymbol{\omega}_o + \boldsymbol{\Omega})}{2} - \frac{3\mathcal{G}M_p}{2} \frac{\mathbf{r}^\top \mathbf{I} \mathbf{r}}{r^5} - U_{\text{self}}(\mathbf{q}). \end{aligned} \quad (170)$$

The Lie momenta associated with  $\boldsymbol{\eta} = (\boldsymbol{\omega}_o, \boldsymbol{\omega}_c, \boldsymbol{\omega}_s)$  are

$$\boldsymbol{\Pi}_o = \frac{\partial L_{\text{go}}}{\partial \boldsymbol{\omega}_o} = \mathbb{I}_o (\boldsymbol{\omega}_o + \boldsymbol{\Omega}), \quad (171)$$

$$\boldsymbol{\Pi}_c = \frac{\partial L_{\text{go}}}{\partial \boldsymbol{\omega}_c} = \mathbb{I}_c (\boldsymbol{\omega}_c + \boldsymbol{\Omega}), \quad (172)$$

$$\boldsymbol{\Pi}_s = \frac{\partial L_{\text{go}}}{\partial \boldsymbol{\omega}_s} = \mathbb{I}_s (\boldsymbol{\omega}_s + \boldsymbol{\Omega}), \quad (173)$$



from which we deduce the Hamiltonian

$$H_{\text{go}}(\mathbf{y}) = \frac{\boldsymbol{\Pi}_c^{\text{T}}(\mathbb{I}_c)^{-1}\boldsymbol{\Pi}_c}{2} + \frac{\boldsymbol{\Pi}_o^{\text{T}}(\mathbb{I}_o)^{-1}\boldsymbol{\Pi}_o}{2} + \frac{\boldsymbol{\Pi}_s^{\text{T}}(\mathbb{I}_s)^{-1}\boldsymbol{\Pi}_s}{2} - \boldsymbol{\Omega}^{\text{T}}(\boldsymbol{\Pi}_c + \boldsymbol{\Pi}_o + \boldsymbol{\Pi}_s) + \frac{3\mathcal{G}M_p}{2} \frac{\mathbf{r}^{\text{T}}\mathbb{I}\mathbf{r}}{r^5} + U_{\text{self}}(\mathbf{q}), \quad (174)$$

which is a function of  $\mathbf{y} = (\boldsymbol{\Pi}_o, \mathbf{y}_c, \mathbf{y}_s)$  with  $\mathbf{y}_i = (\boldsymbol{\Pi}_i, \mathbf{I}_i, \mathbf{J}_i, \mathbf{K}_i)$ . The Poisson matrix  $\mathbf{B}_{\text{go}}(\mathbf{y})$  associated with this set of variables is

$$\mathbf{B}_{\text{go}}(\mathbf{y}) = \begin{bmatrix} \hat{\boldsymbol{\Pi}}_o & \mathbf{0} & \mathbf{0} \\ \mathbf{0} & \mathbf{b}(\mathbf{y}_c) & \mathbf{0} \\ \mathbf{0} & \mathbf{0} & \mathbf{b}(\mathbf{y}_s) \end{bmatrix}, \quad \mathbf{b}(\mathbf{y}_i) = \begin{bmatrix} \hat{\boldsymbol{\Pi}}_i & \hat{\mathbf{I}}_i & \hat{\mathbf{J}}_i & \hat{\mathbf{K}}_i \\ \hat{\mathbf{I}}_i & \mathbf{0} & \mathbf{0} & \mathbf{0} \\ \hat{\mathbf{J}}_i & \mathbf{0} & \mathbf{0} & \mathbf{0} \\ \hat{\mathbf{K}}_i & \mathbf{0} & \mathbf{0} & \mathbf{0} \end{bmatrix}, \quad i = c, s. \quad (175)$$

Although  $\mathbf{y}$  has 27 components, the system evolves in a phase space  $\Sigma_{\text{go}}$  of dimension  $14 = 2 \times 7$  whose degrees of freedom are the three rotations of the central region, the three rotation of the shell and an additional degree of freedom associated with the ocean:

$$\Sigma_{\text{go}} = \{\mathbf{y} \in \mathbb{R}^{27} : C_{\text{go}}^i(\mathbf{y}) = c_i, 0 \leq i \leq 12\} \quad (176)$$

where the thirteen Casimir functions are

$$\begin{aligned} C_{\text{go}}^0(\mathbf{y}) &= \frac{1}{2}\boldsymbol{\Pi}_o^{\text{T}}\boldsymbol{\Pi}_o, & C_{\text{go}}^1(\mathbf{y}) &= \frac{1}{2}\mathbf{I}_c^{\text{T}}\mathbf{I}_c, & C_{\text{go}}^2(\mathbf{y}) &= \frac{1}{2}\mathbf{J}_c^{\text{T}}\mathbf{J}_c, & C_{\text{go}}^3(\mathbf{y}) &= \frac{1}{2}\mathbf{K}_c^{\text{T}}\mathbf{K}_c, \\ C_{\text{go}}^4(\mathbf{y}) &= \mathbf{J}_c^{\text{T}}\mathbf{K}_c, & C_{\text{go}}^5(\mathbf{y}) &= \mathbf{K}_c^{\text{T}}\mathbf{I}_c, & C_{\text{go}}^6(\mathbf{y}) &= \mathbf{I}_c^{\text{T}}\mathbf{J}_c, & C_{\text{go}}^7(\mathbf{y}) &= \frac{1}{2}\mathbf{I}_s^{\text{T}}\mathbf{I}_s, \\ C_{\text{go}}^8(\mathbf{y}) &= \frac{1}{2}\mathbf{J}_s^{\text{T}}\mathbf{J}_s, & C_{\text{go}}^9(\mathbf{y}) &= \frac{1}{2}\mathbf{K}_s^{\text{T}}\mathbf{K}_s, & C_{\text{go}}^{10}(\mathbf{y}) &= \mathbf{J}_s^{\text{T}}\mathbf{K}_s, & C_{\text{go}}^{11}(\mathbf{y}) &= \mathbf{K}_s^{\text{T}}\mathbf{I}_s, \\ C_{\text{go}}^{12}(\mathbf{y}) &= \mathbf{I}_s^{\text{T}}\mathbf{J}_s. \end{aligned} \quad (177)$$

In order to proceed, we have to compute the inverse of the inertia matrix of the ocean  $(\mathbb{I}_o)^{-1}$  for which we are missing the principal basis. The other terms of the Hamiltonian  $H_{\text{go}}$  (Eq. 174) are fully explicit and do not cause any problem. To make the computation analytical, we anticipate the equilibrium point solution

$$\begin{aligned} \boldsymbol{\Pi}_{o,e} &= C_o\boldsymbol{\Omega}\mathbf{k} & \boldsymbol{\Pi}_{s,e} &= C_s\boldsymbol{\Omega}\mathbf{k}, & \mathbf{I}_{s,e} &= \mathbf{i}, & \mathbf{J}_{s,e} &= \mathbf{j}, & \mathbf{K}_{s,e} &= \mathbf{k}, \\ \boldsymbol{\Pi}_{c,e} &= C_c\boldsymbol{\Omega}\mathbf{k}, & \mathbf{I}_{c,e} &= \mathbf{i}, & \mathbf{J}_{c,e} &= \mathbf{j}, & \mathbf{K}_{c,e} &= \mathbf{k}, \end{aligned} \quad (178)$$

where  $C_o = C'_s - C'_c$ . We further define  $A_o = A'_s - A'_c$  and  $B_o = B'_s - B'_c$ . We then expand  $(\mathbb{I}_o)^{-1}$  in Taylor series up to the second order in  $\mathbf{y} - \mathbf{y}_e$ . This is sufficient to get the equations of motion of the linearised system. We verify that  $\mathbf{y}_e$  (Eq. 178) actually is a solution of  $\nabla_{\mathbf{y}}H_{\text{go}}(\mathbf{y}_e) = \sum_i \mu_i \nabla_{\mathbf{y}}C_{\text{go}}^i(\mathbf{y}_e)$  where the Lagrange multipliers are

$$\begin{aligned} \mu_0 &= 0, & \mu_1 &= 3A_c^o\sigma_{xx}^0 + u_{xx}, & \mu_2 &= 3B_c^o\sigma_{yy}^0 + u_{yy}, \\ \mu_3 &= 3C_c^o\sigma_{zz}^0 + (C_c + C'_c)\Omega^2 + u_{zz}, & \mu_4 &= \mu_5 = \mu_6 = 0, & \mu_7 &= 3A_s^o\sigma_{xx}^0 + u_{xx}, \\ \mu_8 &= 3B_s^o\sigma_{yy}^0 + u_{yy}, & \mu_9 &= 3C_s^o\sigma_{zz}^0 + (C_s - C'_s)\Omega^2 + u_{zz}, \\ \mu_{10} &= \mu_{11} = \mu_{12} = 0, \end{aligned} \quad (179)$$

with

$$A_s^o = A_s + A'_s, \quad A_c^o = A_c - A'_c. \quad (180)$$

The same rules apply for  $B_s^o$ ,  $C_s^o$ ,  $B_c^o$  and  $C_c^o$ . Let us write the matrix of the linearised problem in the variables

$$\begin{aligned} \delta \mathbf{y}^* = & \left( \delta \Pi_{s,z}, \delta \Pi_{c,z}, \delta I_{s,y}, \delta I_{c,y}, \delta \Pi_{s,x}, \delta I_{s,z}, \delta \Pi_{c,x}, \delta I_{c,z}, \delta \Pi_{o,x}, \delta \Pi_{s,y}, \right. \\ & \delta J_{s,z}, \delta \Pi_{c,y}, \delta J_{c,z}, \delta \Pi_{o,y}, \delta \Pi_{o,z}, \delta I_{s,x}, \delta J_{s,y}, \delta K_{s,z}, \delta I_{s,y} + J_{s,x}, \delta I_{c,x}, \delta J_{c,y}, \\ & \left. \delta K_{c,z}, \delta I_{c,y} + J_{c,x}, \delta I_{s,z} + K_{s,x}, \delta J_{s,z} + K_{s,y}, \delta I_{c,z} + K_{c,x}, \delta J_{c,z} + K_{c,y} \right)^T, \end{aligned} \quad (181)$$

such that, with the driving perturbation, the system reads

$$\delta \dot{\mathbf{y}}^* - \mathbf{A}_{\text{go}}^*(\mathbf{y}_e) \delta \mathbf{y}^* = \delta \mathbf{z}_{\text{go}}(t), \quad \mathbf{A}_{\text{go}}^*(\mathbf{y}_e) := \left[ \begin{array}{cc|cc|c} \mathbf{0} & -\mathbf{A}_{\text{go}}^{12} & \mathbf{0} & \mathbf{0} & \cdot \\ \mathbf{A}_{\text{go}}^{21} & \mathbf{0} & \mathbf{0} & \mathbf{0} & \cdot \\ \hline \mathbf{0} & \mathbf{0} & \mathbf{0} & -\mathbf{A}_{\text{go}}^{34} & \cdot \\ \mathbf{0} & \mathbf{0} & \mathbf{A}_{\text{go}}^{43} & \mathbf{0} & \cdot \\ \hline \mathbf{0} & \mathbf{0} & \mathbf{0} & \mathbf{0} & \mathbf{0} \end{array} \right], \quad (182)$$

with

$$\mathbf{A}_{\text{go}}^{12} = \begin{bmatrix} 3(B_s^o - A_s^o)(\kappa_1 - \kappa_2) + U_{xy} & -U_{xy} \\ -U_{xy} & 3(B_c^o - A_c^o)(\kappa_1 - \kappa_2) + U_{xy} \end{bmatrix}, \quad (183)$$

$$\mathbf{A}_{\text{go}}^{21} = \begin{bmatrix} \frac{1}{C_s} & 0 \\ 0 & \frac{1}{C_c} \end{bmatrix}, \quad (184)$$

and

$$\mathbf{A}_{\text{go}}^{34} = \begin{bmatrix} -\Omega & M_s^B + U_{yz} + F_{1,s}^B & 0 & -U_{yz} - F_3^B & F_{2,s}^B \\ \frac{1}{B_s} & \frac{C_s - B_s}{B_s} \Omega & 0 & 0 & 0 \\ 0 & -U_{yz} - F_3^B & -\Omega & M_c^B + U_{yz} + F_{1,c}^B & -F_{2,c}^B \\ 0 & 0 & \frac{1}{B_c} & \frac{C_c - B_c}{B_c} \Omega & 0 \\ 0 & -F_{2,s}^B C_o \Omega & 0 & F_{2,c}^B C_o \Omega & -F_4^B - \Omega \end{bmatrix}, \quad (185)$$

$$\mathbf{A}_{\text{go}}^{43} = \begin{bmatrix} -\Omega & M_s^A + U_{xz} + F_{1,s}^A & 0 & -U_{xz} - F_3^A & F_{2,s}^A \\ \frac{1}{A_s} & \frac{C_s - A_s}{A_s} \Omega & 0 & 0 & 0 \\ 0 & -U_{xz} - F_3^A & -\Omega & M_c^A + U_{xz} + F_{1,c}^A & -F_{2,c}^A \\ 0 & 0 & \frac{1}{A_c} & \frac{C_c - A_c}{A_c} \Omega & 0 \\ 0 & -F_{2,s}^A C_o \Omega & 0 & F_{2,c}^A C_o \Omega & -F_4^A - \Omega \end{bmatrix}. \quad (186)$$

In matrices  $\mathbf{A}_{\text{go}}^{34}$  and  $\mathbf{A}_{\text{go}}^{43}$  (Eqs. 185,186), the interaction with the central planet is represented by the terms

$$M_i^A = 3(C_i^o - A_i^o)\kappa_1, \quad M_i^B = 3(C_i^o - B_i^o)\kappa_2, \quad i = s, c, \quad (187)$$

the core/shell gravitational coupling through the ocean interface is given by

$$U_{xy} := u_{xy} + u_{yx} - u_{xx} - u_{yy}, \quad (188)$$

$$U_{xz} := u_{xz} + u_{zx} - u_{xx} - u_{zz}, \quad (189)$$

$$U_{yz} := u_{yz} + u_{zy} - u_{yy} - u_{zz}, \quad (190)$$

From the expressions of  $(u_{ab})_{a,b \in \{x,y,z\}}$  given in Eqs. (158-166), we get

$$U_{xy} = 2\mathcal{G}(B_c^o - A_c^o)(\rho_s(g_s - f_s) + (\rho_o - \rho_s)(g_o - f_o)), \quad (191)$$

$$U_{xz} = 2\mathcal{G}(C_c^o - A_c^o)(\rho_s(h_s - f_s) + (\rho_o - \rho_s)(h_o - f_o)), \quad (192)$$

$$U_{yz} = 2\mathcal{G}(C_c^o - B_c^o)(\rho_s(h_s - g_s) + (\rho_o - \rho_s)(h_o - g_o)). \quad (193)$$

Finally, the remaining terms

$$F_{1,s}^K = \frac{(C'_s - K'_s)(C'_s - K'_s)}{K_o} \Omega^2, \quad K = A, B \quad (194)$$

$$F_{1,c}^K = \frac{(C'_c - K'_c)(C'_c - K'_c)}{K_o} \Omega^2, \quad K = A, B \quad (195)$$

$$F_{2,i}^K = \frac{C'_i - K'_i}{K_o} \Omega, \quad i = s, c, \quad K = A, B \quad (196)$$

$$F_3^K = \frac{(C'_s - K'_s)(C'_c - K'_c)}{K_o} \Omega^2, \quad K = A, B \quad (197)$$

$$F_4^K = \frac{C_o - K_o}{K_o} \Omega, \quad K = A, B \quad (198)$$

are only present in the linearised system because of the rotation of the ocean. If the Casimir  $C_0(\mathbf{y}) = \mathbf{\Pi}_o \cdot \mathbf{\Pi}_o / 2$  were set equal to zero, i.e., if the ocean were not rotating with respect to the inertial frame, all  $F_{1,i}^K$ ,  $F_{2,i}^K$ ,  $F_3^K$ , and  $F_4^K$ , with  $K = A, B$  and  $i = s, c$ , would be nil. The same conclusion would hold if the kinetic energy of the ocean  $\mathbf{\Pi}_o^T (\mathbb{I}_o)^{-1} \mathbf{\Pi}_o / 2$  were skipped from the Hamiltonian  $H_{go}$ . We thus interpret these terms as due to the centrifugal force felt by the ocean and responsible for an additional pressure on the interfaces with the interior and the shell. In that case – i.e., if the kinetic energy of the ocean were dropped –, the ocean angular momentum  $\mathbf{\Pi}_o$  would be decoupled from the rest of the system. A quick inspection of the last row and column of the matrices  $\mathbf{A}_{go}^{34}$  and  $\mathbf{A}_{go}^{43}$  indeed shows that a perturbation of  $\mathbf{\Pi}_o$  would rotate at the eigenfrequency  $\Omega$  with respect to the laboratory frame, and would thus be fixed in the inertial frame.

We note that given the structure of the matrix  $\mathbf{A}_{go}^*$ , the linearised system is characterised by two libration frequencies in longitude and five frequencies associated with libration in latitude and wobble.

For this problem, the Lyapunov function reads

$$\begin{aligned}
N_{\text{go}}(\mathbf{y}) = & \\
& \frac{1}{2A_o} \left( \Pi_{o,x} - \frac{1}{2}(C'_c - A'_c)\Omega(I_{c,z} - K_{c,x}) + \frac{1}{2}(C'_s - A'_s)\Omega(I_{s,z} - K_{s,x}) \right)^2 \\
& + \frac{1}{2B_o} \left( \Pi_{o,y} - \frac{1}{2}(C'_c - B'_c)\Omega(J_{c,z} - K_{c,y}) + \frac{1}{2}(C'_s - B'_s)\Omega(J_{s,z} - K_{s,y}) \right)^2 \\
& + \frac{1}{2A_c} \left( \Pi_{c,x} + \frac{1}{2}(C_c - A_c)\Omega(I_{c,z} - K_{c,x}) \right)^2 \\
& + \frac{1}{2B_c} \left( \Pi_{c,y} + \frac{1}{2}(C_c - B_c)\Omega(J_{c,z} - K_{c,y}) \right)^2 + \frac{1}{2C_c} \Pi_{c,z}^2 \\
& + \frac{1}{2A_s} \left( \Pi_{s,x} + \frac{1}{2}(C_s - A_s)\Omega(I_{s,z} - K_{s,x}) \right)^2 \\
& + \frac{1}{2B_s} \left( \Pi_{s,y} + \frac{1}{2}(C_s - B_s)\Omega(J_{s,z} - K_{s,y}) \right)^2 + \frac{1}{2C_s} \Pi_{s,z}^2 \\
& + \frac{U_{xy}}{4} ((I_{c,y} - J_{c,x}) - (I_{s,y} - J_{s,x}))^2 + \frac{U_{xz}}{4} ((I_{c,z} - K_{c,x}) - (I_{s,z} - K_{s,x}))^2 \\
& + \frac{U_{yz}}{4} ((J_{c,z} - K_{c,y}) - (J_{s,z} - K_{s,y}))^2 \\
& + \frac{n_1^s}{2} (J_{s,x} - I_{s,y})^2 + \frac{n_2^s}{2} (I_{s,z} - K_{s,x})^2 + \frac{n_3^s}{2} (J_{s,z} - k_{s,y})^2 \\
& + \frac{n_1^c}{2} (J_{c,x} - I_{c,y})^2 + \frac{n_2^c}{2} (I_{c,z} - K_{c,x})^2 + \frac{n_3^c}{2} (J_{c,z} - k_{c,y})^2,
\end{aligned} \tag{199}$$

with

$$\begin{aligned}
n_1^* &= \frac{3}{4}(B_*^o - A_*^o)(\kappa_1 - \kappa_2), & n_2^* &= \frac{1}{4}(C_*^o - A_*^o)(\Omega^2 + 3\kappa_1), \\
n_3^* &= \frac{1}{4}(C_*^o - B_*^o)(\Omega^2 + 3\kappa_2),
\end{aligned} \tag{200}$$

and where  $* = s, c$ . We deduce that the system is nonlinearly stable if the following conditions are met

$$U_{xy} > 0, \quad U_{xz} > 0, \quad U_{yz} > 0, \quad C_*^o > B_*^o > A_*^o \quad \text{with } * = s, c. \tag{201}$$

Using the expressions of  $U_{xy}$ ,  $U_{xz}$ , and  $U_{yz}$  (Eqs. 191-193) expanded at first order in the equatorial and polar flatness, the conditions (201) are equivalent to

$$\begin{cases} \rho_s \frac{a_s - c_s}{a_s} + (\rho_o - \rho_s) \frac{a_o - c_o}{a_o} > \rho_s \frac{a_s - b_s}{a_s} + (\rho_o - \rho_s) \frac{a_o - b_o}{a_o} > 0, \\ C_*^o > B_*^o > A_*^o, & * = s, c. \end{cases} \tag{202}$$

**Table 2** Orbital and physical parameters of Io taken from (Noyelles, 2014).

Parameter	value	units
$\mathcal{G}M_p$ (Jupiter)	126 712 765	$\text{km}^3/\text{s}^2$
$a$	422 029.958	km
$e$	0.00415	
$i$	2.16	arcmin
$\Omega$	1297.204 472 527 9755	rad/a
$A/(mR^2)$	0.375 127	
$B/(mR^2)$	0.377 342	
$C/(mR^2)$	0.378 080	
$A_c/(mR^2)^a$	0.006 007 5578	
$B_c/(mR^2)^a$	0.006 283 9600	
$C_c/(mR^2)^a$	0.006 253 4432	

<sup>a</sup> Moments of inertia of the core computed from the internal model 1 of (Noyelles, 2014).

**Table 3** Eigenperiods of Io's rotational motion (Eq. 204).

source	$T_u$ (day)	$T_v$ (day)	$T_w$ (day)	$T_z$ (day)
Noyelles (2014)	13.2322	166.3520	225.0927	1.7382
This work: model fc (Sect. 4.1)	13.2504	157.2780	224.5395	1.7385
This work: model fc' (Sect. 4.2)	13.2502	156.5653	224.5402	1.7368

Finally, as in the previous section, to get the forced solution, we decompose the driving excitation  $\delta\mathbf{z}_{\text{go}}(t)$  as  $(\delta\mathbf{z}_{\text{go}}^1, \delta\mathbf{z}_{\text{go}}^2, \mathbf{0})$ , with

$$\delta\mathbf{z}_{\text{go}}^1(t) = \begin{pmatrix} 3(B_s^o - A_s^o)\sigma_{xy}^1 \\ 3(B_c^o - A_c^o)\sigma_{xy}^1 \\ 0 \\ 0 \end{pmatrix}, \quad \delta\mathbf{z}_{\text{go}}^2(t) = \begin{pmatrix} 3(C_s^o - B_s^o)\sigma_{yz}^1 \\ 0 \\ 3(C_c^o - B_c^o)\sigma_{yz}^1 \\ 0 \\ 0 \\ -3(C_s^o - A_s^o)\sigma_{xz}^1 \\ 0 \\ -3(C_c^o - A_c^o)\sigma_{xz}^1 \\ 0 \\ 0 \end{pmatrix}. \quad (203)$$

## 6 Application

### 6.1 Io's libration modes

Io, one of the Galilean satellite of Jupiter, is assumed to have a liquid core (Anderson et al., 1996). Its rotation motion has already been studied within the Poincaré-Hough paradigm using a Hamiltonian formalism (Henrard, 2008). This analysis has then been extended using the same method in (Noyelles, 2013, 2014). Although the approach in *ibid.* is Hamiltonian, it differs from that described in Sect. 4 which is expressed in non-canonical variables. Here, we revisit the problem with the aim of validating our method and, more specifically, the quasi-spherical approximation (Sect. 4.2).

The orbital and physical parameters of Io, which are summarised in Tab. 2, are taken from (Noyelles, 2013, 2014)<sup>2</sup>. The eigenfrequencies  $\omega_u$ ,  $\omega_v$ ,  $\omega_w$  and  $\omega_z$  are directly computed from the matrix  $\mathbf{A}_{\text{fc}}^*$  (Eqs. 132,133) for the Poincaré-Hough model (Sect. 4.1), and from the matrix  $\mathbf{A}_{\text{fc}'}^*$  (Eqs. 146,147) for the quasi-spherical approximation (Sect. 4.2). Hereafter, the two models are referred to as “model fc” and “model fc’”, respectively. The eigenfrequencies are then converted into periods for a direct comparison with (Noyelles, 2014). The correspondence between the eigenperiods of *ibid.* and the eigenfrequencies of this work is

$$T_u = \frac{2\pi}{\omega_u}, \quad T_v = \frac{2\pi}{\omega_v - \Omega}, \quad T_w = \frac{2\pi}{\omega_w}, \quad T_z = \frac{2\pi}{\omega_z}. \quad (204)$$

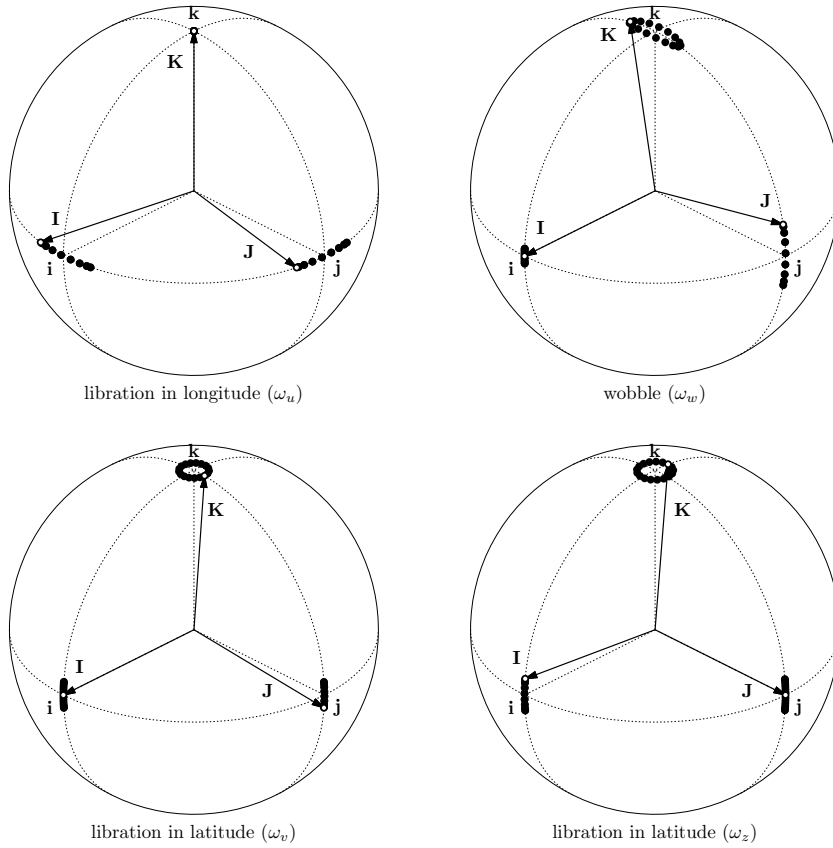
The results are gathered in Tab. 3. We observe a good match between model fc and that of (Noyelles, 2014) for  $T_u$ ,  $T_w$ , and  $T_z$  with a maximal error of about 0.2%. There is a larger discrepancy between the two approaches in the case of  $T_v$  with a deviation of almost 6%, but this eigenmode is more sensitive due to the small denominator  $\omega_v - \Omega$  (Eq. 204). It is also very sensitive to the polar flattening of the core (Noyelles, 2012). Nevertheless, the agreement is satisfactory given that the methods to compute the eigenperiods in both studies are very different. The eigenfrequencies given by models fc and fc’ are also very close to each other. Once again, the largest discrepancy occurs for  $T_v$ , but here it does not exceed 0.5%. We thus conclude that the quasi-spherical approximation is justified.

Figure 2 represents the trajectories of the principal axes  $\mathbf{I}$ ,  $\mathbf{J}$ , and  $\mathbf{K}$  in the laboratory frame  $(\mathbf{i}, \mathbf{j}, \mathbf{k})$  while the system stands in each of the eigenmodes. The corresponding eigenfrequencies are recalled below each subfigure. We recognise the libration motions of a rigid satellite which the name of the eigenmodes have been taken from. In (Henrard, 2008) and in (Noyelles, 2013, 2014), the eigenmode associated with  $\omega_z$  is referred to as the free libration of the core. Nevertheless, given the strong similarity between the motions associated with  $\omega_v$  and  $\omega_z$ , we chose to attribute the same name “libration in latitude” for both of them. Furthermore, from the observation of the surface only it is hardly possible to distinguish one from the other. Actually, the distinction between the two modes lies in the relative position of  $\mathbf{\Pi}_c$  and  $\mathbf{\Pi}$ , as shown in Fig. 3. When the satellite is in the eigenmode associated with  $\omega_v$ , the two vectors are on the same side from the origin, while in the eigenmode of frequency  $\omega_z$  they are on opposite side.

## 6.2 Titan’s equilibrium obliquity

In this section, we analyse the rotation of Titan orbiting Saturn. Several hints suggest that this satellite holds a global ocean under its surface (Coyette et al., 2016, and references therein). Among these clues, an important one for our purpose is Titan’s “high” obliquity of  $0.32^\circ$  which could not be explained if the satellite were solid (Bills and Nimmo, 2011). Nevertheless, a discrepancy still persists between the observations and the expected obliquity associated with the Cassini state, the latter remaining below  $0.15^\circ$  for a large class of interior models (e.g., Baland et al., 2011). Therefore, it has been proposed that Titan’s current obliquity is amplified

<sup>2</sup> Here and throughout the paper, we follow the IAU recommendations which state that the symbol for a Julian year is “a”. Hence, radian per year is written “rad/a”.



**Fig. 2** Eigenmodes of Io’s rotation motion computed with the parameters of Tab. 2. Positions at constant time intervals of the principal axes (**I**, **J**, **K**) are depicted by black dots. Open circles indicate the initial condition. Intersections of the dotted great circles of the unit sphere represent the laboratory frame (**i**, **j**, **k**). Jupiter is in the direction of the vector **i**. The associated eigenfrequencies are recalled below each figure.

by a resonance with one of the remaining orbital forcing frequencies (Baland et al., 2011; Noyelles and Nimmo, 2014).

In his abstract, Henrard (2008) wrote about Io that “the addition of a degree of freedom (the spin of the core) with a frequency close to the orbital frequency multiplies the possibility of resonances”. In the case of Titan, we also have an additional degree of freedom in comparison to the previous studies quoted above. We thus expect our model to be able to tilt Titan’s axis more easily.

The orbital elements of Titan are taken from the ephemeris TASS1.6 (Vienne and Duriez, 1995). From the full solution, we only retain the keplerian motion and the nodal precession of the orbit with respect to the Laplace plane<sup>3</sup>. These parameters are summarised in Tab. 4. Regarding Titan internal structure, we

<sup>3</sup> Here, we define Titan’s Laplace plane as the plane whose orientation is given by the constant part of the inclination solution of TASS1.6. (Vienne and Duriez, 1995)

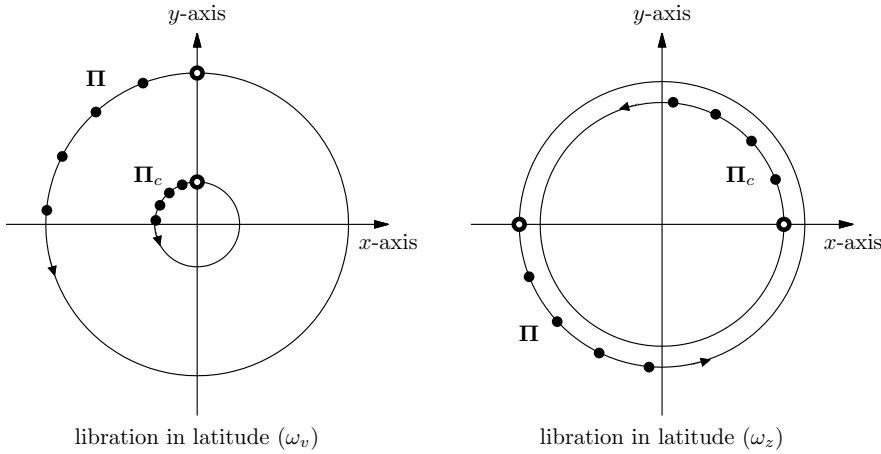


**Fig. 3** Trajectories of the projections of  $\Pi$  and  $\Pi_c$  on the plane  $(i, j)$  while Io is in libration in latitude. Dots represent successive positions of the vectors. Open circles denote the initial conditions. In the eigenmode with frequency  $\omega_v$ , the two vectors are on the same side from the origin whereas in the eigenstate of frequency  $\omega_z$ , they are on opposite side. The radial coordinate of each vector is plotted in a log scale with arbitrary units. These figures have been computed using Io's parameters (cf Tab. 2).

select two models proposed by Fortes (2012), hereafter referred to as model F1 and F2. They assume a global ocean with extreme densities equal to  $1023 \text{ kg/m}^3$  and  $1281 \text{ kg/m}^3$ , respectively. In model F1, the ocean is a mixture of water and methanol, while in model F2, the ocean is made of water and ammonia. Parameters of these interior models are summarised in Tab. 5. In both models, the average density is  $1881 \text{ kg/m}^3$  and the mean moment of inertia  $I/(mR^2)$  remains within the errorbars provided by Less et al. (2012). The equatorial flattening  $\zeta$  is obtained by integration of Clairaut's equation (Clairaut, 1743) assuming an hydrostatic equilibrium (same as Richard, 2014). The boundary semi-axes at volumetric mean radius  $R$  between two layers are given by (e.g., Rambaux and Castillo-Rogez, 2013)

$$a = R \left( 1 + \frac{7}{9}\zeta \right), \quad b = R \left( 1 - \frac{2}{9}\zeta \right), \quad c = R \left( 1 - \frac{5}{9}\zeta \right). \quad (205)$$

The values of the derived parameters involved in the Hamiltonian  $H_{\text{go}}(\mathbf{y})$  (Eq. 174) are listed in Tab. 6.

The eigenfrequencies computed for the two interior models F1 and F2 are shown in Tab. 7. For each model, we assume either a rotating or a static ocean with respect to the inertial frame (see Sect. 5). For reference, we also provide the eigenfrequencies assuming a fully rigid satellite. To interpret these eigenfrequencies, the associated trajectories of the vectors  $(\mathbf{I}_c, \mathbf{J}_c, \mathbf{K}_c)$  and  $(\mathbf{I}_s, \mathbf{J}_s, \mathbf{K}_s)$  are displayed in Fig. 4. We recognise librations in longitude at  $\omega_{u1}$  and  $\omega_{u2}$ , librations in latitude at  $\omega_{v1}$ ,  $\omega_{v2}$  and  $\omega_{v3}$ , and wobbles at  $\omega_{w1}$  and  $\omega_{w2}$ . From Tab. 7, we observe that each eigenmode has a specific range of frequencies. Libration frequencies in latitude are close to the mean motion  $\Omega \approx 143.9240 \text{ rad/a}$ . Frequencies of libration in longitude are between 2 and 8 rad/a, and the wobble is the slowest motion with frequencies ranging between 0.01 and 0.2 rad/a.



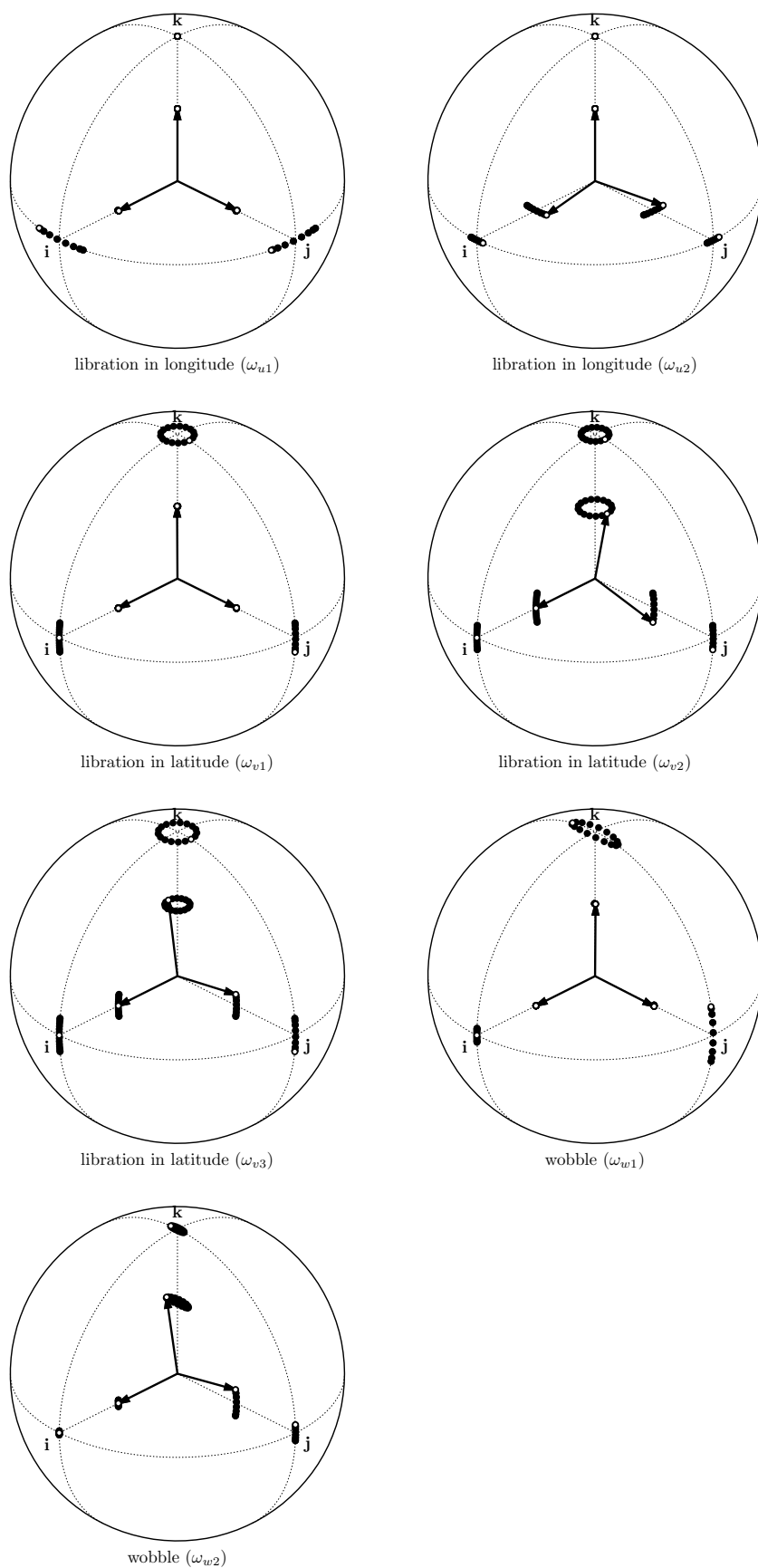


**Fig. 4** Eigenmodes of Titan's rotation motion computed with the interior model F1. Positions at constant time intervals of the shell principal axes ( $\mathbf{I}_s, \mathbf{J}_s, \mathbf{K}_s$ ) are depicted by black dots on the unit sphere. Those of the interior ( $\mathbf{I}_c, \mathbf{J}_c, \mathbf{K}_c$ ) are plotted at half the radius of the unit sphere. The white dots indicate the initial condition. Intersections of the dotted great circles of the unit sphere represent the laboratory frame ( $\mathbf{i}, \mathbf{j}, \mathbf{k}$ ). Saturn is in the direction of the vector  $\mathbf{i}$ . The associated eigenfrequencies are recalled below each figure.

**Table 4** Orbital parameters of Titan used in this study.

Parameter	value	units	reference
$\mathcal{G}M_p$ (Saturn)	37 931 272	km <sup>3</sup> /s <sup>2</sup>	(Campbell and Anderson, 1989)
$a$	1 221 729	km	computed <sup>a</sup>
$e$	0.028		(Vienne and Duriez, 1995)
$i^b$	0.320	deg	(Vienne and Duriez, 1995)
$\Omega$	143.924 047 85	rad/a	(Vienne and Duriez, 1995)
$d\Phi/dt$	-0.008 931 24	rad/a	(Vienne and Duriez, 1995)

<sup>a</sup> The semimajor axis has been computed from the masses of Saturn and Titan given by Campbell and Anderson (1989) and the orbital parameters  $N_6$  and  $p_{06}$  provided by Vienne and Duriez (1995).

<sup>b</sup> Inclination with respect to the Laplace plane given by the amplitude of the second harmonic of  $\zeta_{06}$  in the notation of Vienne and Duriez (1995).

**Table 5** Physical parameters of the two interior models of Titan considered in this study taken from (Fortes, 2012).

Layer	F1			F2		
	$\rho$ (kg/m <sup>3</sup> )	$R$ (km)	$\zeta$ (10 <sup>-5</sup> )	$\rho$ (kg/m <sup>3</sup> )	$R$ (km)	$\zeta$ (10 <sup>-5</sup> )
Ice	930.9	2575	12.068	930.9	2575	12.080
Ocean	1023.5	2475	11.878	1281.3	2475	11.887
Ice V	1272.7	2225	11.552	1350.9	2225	11.488
Ice VI	1338.9	2163	11.521	-	-	-
Silicate	2542.3	2116	11.514	2650.4	1984	11.310

For each layer,  $\rho$  is the density and  $R$  and  $\zeta$  respectively denote the mean radius and the equatorial flattening of the upper boundary.

The condition for Titan to have a significant (shell) obliquity is that one of the libration frequencies in latitude gets close to the excitation frequency of the perturbation  $\sigma_{xz}^1(t)$  (Eq. 69), namely,  $\omega_{xz}^1 = \Omega - \dot{\Phi} \approx 143.9330$  rad/a. In the case of a rigid satellite there is no lever arm. The libration frequency only depends on the total moments of inertia which are constrained by observations. This frequency, equal to 143.9582 rad/a, leads to an obliquity of 0.113° which is about one third of the actual value  $\varepsilon_{\text{obs}} = 0.32^\circ$ .

When the ocean is taken into account, the system has three distinct frequencies of libration in latitude which can potentially be in resonance with the orbital precession rate. It should nevertheless be stressed that when the rotation of the ocean is set to zero, the frequency  $\omega_{w3}$  in Tab. 7 is just the mean motion  $\Omega$  which is not involved in the tilting of the shell axis. Titan’s obliquities  $\varepsilon$  computed with the different models are gathered in Tab. 8. Note that we allow the obliquity to be negative as explained in Fig. 5. As expected, within the “static ocean” hypothesis the ocean is not affected by the perturbation  $\sigma_{xz}^1$ . Its obliquity is  $\varepsilon_o = -i$ , meaning that  $\mathbf{\Pi}_o$  remains aligned with the Laplace pole  $\mathbf{k}$  which is the third axis of our laboratory reference frame. The last two eigenfrequencies  $\omega_{v1}$  and  $\omega_{v2}$  are further away from  $\omega_{xz}^1$  than  $\omega_{v3}$ . They only produce a shell obliquity of  $\varepsilon_s \approx 0.06^\circ$  which is much lower than the observed one. Furthermore, this result does not significantly vary from model F1 to model F2.

If the rotation of the ocean is set equal to the mean rotation of the satellite,  $\omega_{w3}$  is the eigenfrequency responsible for the tilt of Titan’s shell spin pole. With the two models F1 and F2 considered here, the results are still very low:  $\varepsilon_s = 0.004^\circ$

**Table 6** Derived parameters for Titan’s model.

Parameter	model <b>F1</b>	model <b>F2</b>	units
$A_c/(mR^2)$	0.232 133 9588	0.213 354 6838	
$B_c/(mR^2)$	0.232 160 7420	0.213 379 0654	
$C_c/(mR^2)$	0.232 169 6677	0.213 387 1908	
$A_m/(mR^2)$	0.035 565 0464	0.035 556 8942	
$B_m/(mR^2)$	0.035 569 6492	0.035 561 5041	
$C_m/(mR^2)$	0.035 571 1830	0.035 563 0404	
$A'_c/(mR^2)$	0.104 835 1592	0.131 211 1289	
$B'_c/(mR^2)$	0.104 847 2721	0.131 226 2055	
$C'_c/(mR^2)$	0.104 851 3089	0.131 231 2299	
$A'_m/(mR^2)$	0.178 538 4650	0.223 457 6674	
$B'_m/(mR^2)$	0.178 559 6760	0.223 484 2365	
$C'_m/(mR^2)$	0.178 566 7448	0.223 493 0909	
$u_{xx}/(mR^2)$	135.969 642 03	109.837 900 34	1/day <sup>2</sup>
$u_{xy}/(mR^2)$	135.989 307 93	109.853 755 74	1/day <sup>2</sup>
$u_{xz}/(mR^2)$	135.995 863 22	109.859 040 86	1/day <sup>2</sup>
$u_{yx}/(mR^2)$	135.938 311 45	109.813 022 76	1/day <sup>2</sup>
$u_{yy}/(mR^2)$	135.957 972 82	109.828 874 57	1/day <sup>2</sup>
$u_{yz}/(mR^2)$	135.964 526 60	109.834 158 49	1/day <sup>2</sup>
$u_{zx}/(mR^2)$	135.927 870 23	109.804 732 03	1/day <sup>2</sup>
$u_{zy}/(mR^2)$	135.947 530 09	109.820 582 64	1/day <sup>2</sup>
$u_{zz}/(mR^2)$	135.954 083 36	109.825 866 17	1/day <sup>2</sup>

Note that the number of digits provided in this table is required to recover the values presented in Tabs. 7 and 8.

**Table 7** Eigenfrequencies of Titan’s rotation in rad/a.

	rotating ocean		static ocean		rigid <b>F1/F2</b>	type of motion
	<b>F1</b>	<b>F2</b>	<b>F1</b>	<b>F2</b>		
$\omega_{u1}$	7.9237	8.2656	7.9237	8.2656	2.7117	libration in longitude
$\omega_{u2}$	2.3950	2.1147	2.3950	2.1147		
$\omega_{v1}$	144.3272	144.3641	144.2507	144.2683	143.9582	libration in latitude
$\omega_{v2}$	143.9494	143.9445	143.9528	143.9472		
$\omega_{v3}$	143.9307	143.9266	143.924 <sup>a</sup>	143.924 <sup>a</sup>		
$\omega_{w1}$	0.1943	0.2105	0.1177	0.1104	0.0228	wobble
$\omega_{w2}$	0.0178	0.0138	0.0214	0.0199		

<sup>a</sup> In the case where the ocean is assumed static,  $\omega_{v3} = 143.9240$  rad/a is the mean motion  $\Omega$ .

with model F1 and  $\varepsilon_s = 0.108^\circ$  with model F2. However, the two values vary by a factor 27. A modification of Titan’s interior is thus more likely to produce the observed obliquity if the rotation of the ocean is taken into account.

To illustrate this statement, we generate a series of interior models of Titan based on the model F1. To simulate inhomogeneities in the shell, we slightly modify the equatorial flattening  $\zeta_s$  of the surface from  $11.890 \times 10^{-5}$  to the hydrostatic value  $12.068 \times 10^{-5}$  given in Tab. 5. These numbers should be compared to the

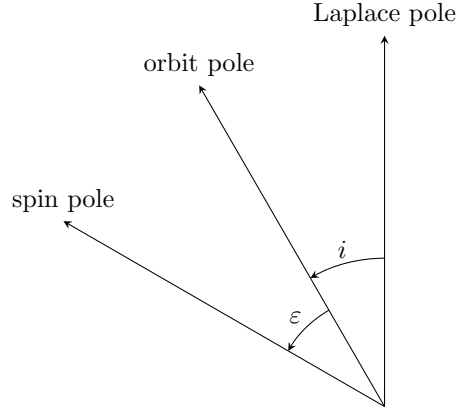


**Fig. 5** Definition of Titan’s inclination  $i$  and obliquity  $\varepsilon$ . In a Cassini state of the averaged problem, the Laplace pole, the orbit pole and the spin pole are in a same plane. We define the orientation of this plane by the inclination measured from the Laplace pole to the orbit pole which by convention is positive. This allows to defined the obliquity as a signed angle measured from the orbit pole to the spin axis. In this figure,  $\varepsilon$  is positive.

**Table 8** Obliquity of Titan’s layers in degree.

	rotating ocean		static ocean		rigid
	<b>F1</b>	<b>F2</b>	<b>F1</b>	<b>F2</b>	<b>F1/F2</b>
core	0.294	0.272	0.149	0.207	0.113
ocean	-0.479	0.208	-0.320	-0.320	0.113
shell	0.004	0.108	0.062	0.064	0.113

The meaning of the sign of the obliquity is explained in Fig. 5.

equatorial flattenings computed with the two models provided by [Iess et al. \(2012\)](#), i.e.,  $11.911 \times 10^{-5}$  (SOL2) and  $12.005 \times 10^{-5}$  (SOL1a). To keep the global moments of inertia constant, the equatorial flattening of all the other layers are refitted using Clairaut’s equation. It has been checked that all these models are nonlinearly stable according to the condition Eq. (202). Figure 6 displays the evolution of the libration frequencies in latitude  $\omega_{v2}$  and  $\omega_{v3}$  as a function of the surface equatorial flattening  $\zeta_s$ . When the rotation of the ocean is considered (left plots),  $\omega_{v3}$  varies sufficiently to cross the resonant frequency  $\omega_{xz}^1$  at  $\zeta_s \approx 11.97 \times 10^{-5}$  where, in the linear approximation, the shell obliquity diverges. More interestingly, for  $\zeta_s \approx 11.94 \times 10^{-5}$ , the driven shell obliquity  $\varepsilon_s$  is equal to the observed value  $\varepsilon_{\text{obs}} = 0.32^\circ$ . In comparison, when the ocean is assumed to be static (right plots of Fig. 6),  $\omega_{v3}$  remains strictly equal to  $\Omega$  and  $\omega_{v2}$  barely evolves. As a consequence, the equilibrium shell obliquity remains practically constant close to  $0.062^\circ$ .

## 7 Conclusion

This paper provides a general method for analysing the rotation dynamics of a rigid body with a fluid internal layer. The study is performed in a non-canonical

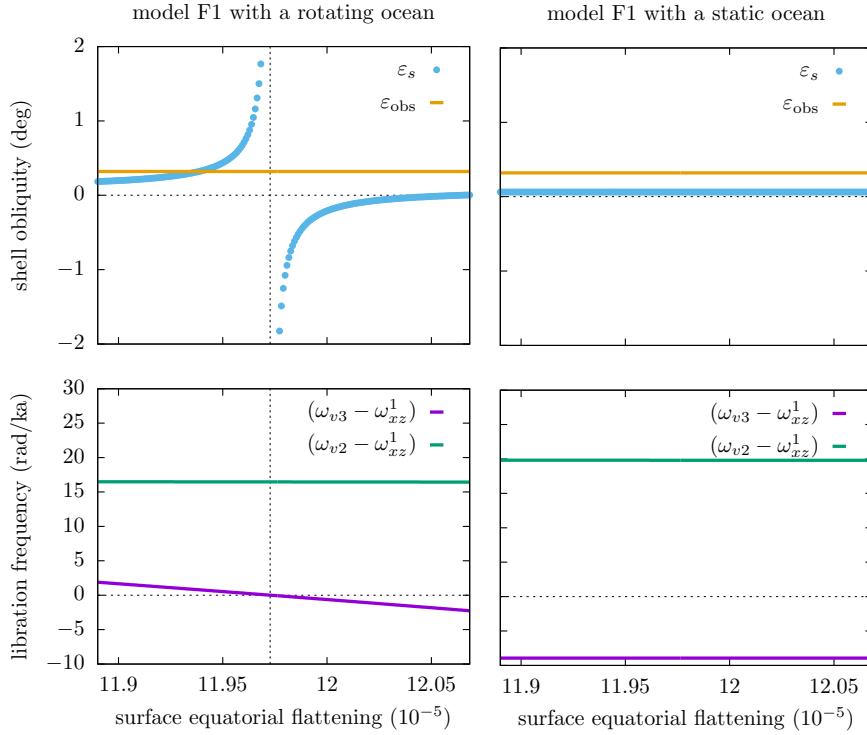


**Fig. 6** Obliquity and libration frequencies as a function of the surface equatorial flattening assuming a rotating ocean (left) or a static ocean (right). The vertical dashed line indicates the location of the resonance  $\omega_{v3} = \omega_{xz}^1$ . In the upper plots,  $\varepsilon_s$  represents the obliquity of the shell at the Cassini state and  $\varepsilon_{\text{obs}}$  the observed value.

Hamiltonian formalism well adapted to systems near relative equilibria such as synchronous satellites in a Cassini state. The Poisson structure of the non-canonical Hamiltonian is here obtained by a Legendre transformation of the corresponding Lagrangian written using Poincaré’s formalism which makes use of the properties of the Lie group acting on the configuration space.

With this approach, we have been able to treat the case of a satellite with a liquid core or with a global underneath ocean in the exact same manner as that of a rigid satellite. All the difficulty is in the calculation of the Lagrangian function – and more specifically, of the kinetic energy of the fluid layer – in terms of generalised coordinates and Lie velocities. For a satellite with a liquid core, Poincaré introduced the concept of a fluid simple motion which cannot be rigorously transposed to a satellite with an ocean. Nevertheless, at first order this fluid layer behaves like a rigid body for which the kinetic energy is known. Tests on a satellite with a liquid core, assuming Io’s physical and orbital parameters, have shown that the errors induced by this approximation do not exceed 0.5% on the eigenfrequencies.

The analysis of a hollow satellite with a fluid core leads to a four degree of freedom dynamical model. The linearised problem in the vicinity of the synchronous

equilibrium state is thus characterised by four eigenmodes. These are a libration in longitude, a wobble and two librations in latitude. To this solved problem, we have provided an analytical expression of the linearised equations written in terms of intuitive variables, namely the components of the angular momenta and of the base frame vectors. We also have clearly identified the fourth eigenmode as a libration in latitude.

The rotation dynamics of a satellite with a global subsurface ocean is governed by seven eigenmodes associated with the seven degrees of freedom of the problem, six of which being equally shared by the interior and the outer shell and the last one being brought by the ocean. Near the synchronous equilibrium state, these eigenmodes are identified as two librations in longitude, two wobbles and three librations in latitude. The amplitude of the third libration in latitude would only vanish if the ocean were static with respect to the inertial frame.

Our study has been motivated by Titan's obliquity measured by the Cassini-Huygens mission. Thus far, dynamical models struggle to explain its high value under the hydrostatic shape hypothesis suggested by the ratio of its Stokes coefficients  $J_2/C_{22} \approx 10/3$ . Here, we show that the rotation of the ocean makes the dynamical model much more sensitive to small perturbations of the interior model than when the ocean is assumed static. As an example, starting from a body in perfect hydrostatic equilibrium, we slightly modified the equatorial flattening of the shell by about 1% of the nominal value. This was enough to bring the obliquity of the Cassini state even beyond the radiometric value with the seven degree of freedom model while the same quantity computed with the static ocean hypothesis remained practically constant scarcely reaching a 0.1% increase.

This work is intended to demonstrate the capability of the seven degree of freedom dynamical model to explain the observed high obliquity of Titan. The problem has therefore been intentionally simplified. Tidal deformations, atmospheric torques, and all orbital perturbations but the main precession relative to the Laplace plane have been discarded. These additions would be required for an exhaustive search of the interior models compatible with the measurements made by the Cassini-Huygens mission: the rotation state, the gravity field coefficients, the shape, the tidal Love number, and the electric field. But this is beyond the scope of the present paper and shall be discussed elsewhere.

**Acknowledgements** We thank Benoît Noyelles and the anonymous referee for their constructive comments. G.B. also thank Philippe Robutel for the useful conversations on the theoretical parts of this work and Rose-Marie Baland and Marie Yseboodt for our instructive discussion on this problem during the 2017 DDA meeting in London.

## References

- Anderson J. D., Sjogren W. L., Schubert G.: Galileo Gravity Results and the Internal Structure of Io. *Science* **272**, 709–712 (1996)
- Baland R.-M., van Hoolst T., Yseboodt M., Karatekin Ö.: Titan's obliquity as evidence of a subsurface ocean? *Astron. Astrophys.* **530**:A141 (2011)
- Baland R.-M., Tobie G., Lefèvre A., Van Hoolst T.: Titan's internal structure inferred from its gravity field, shape, and rotation state. *Icarus* **237**, 29–41 (2014)
- Beck J. A., Hall C. D.: Relative Equilibria of a Rigid Satellite in a Circular Keplerian Orbit. *The Journal of the Astronautical Sciences* **46**(3), 215–247 (1998)

- Béghin C., Randriamboarison O., Hamelin M., et al.: Analytic theory of Titan's Schumann resonance: Constraints on ionospheric conductivity and buried water ocean. *Icarus* **218**, 1028–1042 (2012)
- Bills B. G., Nimmo F.: Rotational dynamics and internal structure of Titan. *Icarus* **214**, 351–355 (2011)
- Campbell J. K., Anderson J. D.: Gravity field of the Saturnian system from Pioneer and Voyager tracking data. *Astronom. J.* **97**, 1485–1495 (1989)
- Clairaut A.: *Théorie de la figure de la Terre*. Davis fils, Paris (1743)
- Colombo G.: Cassini's second and third laws. *Astronom. J.* **71**, 891 (1966)
- Coyette A., Van Hoolst T., Baland R.-M., Tokano T.: Modeling the polar motion of Titan. *Icarus* **265**, 1–28 (2016)
- Dumberry M., Wicczorek M. A.: The forced precession of the Moon's inner core. *Journal of Geophysical Research (Planets)* **121**, 1264–1292 (2016)
- Fortes A. D.: Titan's internal structure and the evolutionary consequences. *Planetary and Space Science* **60**, 10–17 (2012)
- Grasset O., Sotin C.: The Liquidus of H<sub>2</sub>O-NH<sub>3</sub> up to 1.5 GPa: Implications for the Presence of a Liquid Shell in Titan's Interior. In: *Lunar and Planetary Science Conference, Lunar and Planetary Inst. Technical Report*, vol **27** (1996)
- Hall C. D., Beck J. A.: Hamiltonian mechanics and relative equilibria of orbiting gyrostats. *Journal of the Astronautical Sciences* **55**, 53–65 (2007)
- Hansen P. A.: *Entwicklung des Products einer Potenz des Radius Vectors mit dem Sinus oder Cosinus eines vielfachen der wahren Anomalie in Reihen* (in German), *Abhandlungen der Königlich Sachsische Gesellschaft der Wissenschaften*, vol **IV**, Leipzig Hirzel, pp 182–281 (1855)
- Henrard J.: The rotation of Io with a liquid core. *Celestial Mechanics and Dynamical Astronomy* **101**, 1–12 (2008)
- Hough S. S.: The oscillations of a rotating ellipsoidal shell containing fluid. *Philosophical Transactions of the Royal Society of London* **186**, 469–506 (1895)
- Iess L., Jacobson R. A., Ducci M., et al.: The Tides of Titan. *Science* **337**, 457 (2012)
- Laplace P.-S.: *Traité de mécanique céleste - Tome 2*, Chapt 1. Crapelet, Paris (1798)
- Lewis J. S.: Satellites of the Outer Planets: Their Physical and Chemical Nature. *Icarus* **15**, 174–185 (1971)
- Maciejewski A. J.: Reduction, Relative Equilibria and Potential in the Two Rigid Bodies Problem. *Celestial Mechanics and Dynamical Astronomy* **63**, 1–28 (1995)
- Maddocks J. H.: On the Stability of Relative Equilibria. *IMA Journal of Applied Mathematics* **46**(1-2), 71–99 (1991)
- Mathews P. M., Buffett B. A., Herring T. A., Shapiro I. I.: Forced nutations of the earth: Influence of inner core dynamics. I - Theory. II - Numerical results and comparisons. III - Very long interferometry data analysis. *Journal of Geophysical Research* **96**, 8219–8257 (1991)
- Meriggiola R., Iess L.: A new rotational model of Titan from Cassini SAR data. In: *European Planetary Science Congress 2012*, pp EPSC2012–593 (2012)
- Meriggiola R., Iess L., Stiles B. W., et al.: The rotational dynamics of Titan from Cassini RADAR images. *Icarus* **275**, 183–192 (2016)
- Nimmo F., Hamilton D. P., McKinnon W. B., et al.: Reorientation of Sputnik Planitia implies a subsurface ocean on Pluto. *Nature* **540**, 94–96 (2016)
- Noyelles B.: Behavior of nearby synchronous rotations of a Poincaré-Hough satellite at low eccentricity. *Celestial Mechanics and Dynamical Astronomy* **112**, 353–383 (2012)
- Noyelles B.: The rotation of Io predicted by the Poincaré-Hough model. *Icarus* **223**, 621–624 (2013)
- Noyelles B.: *Contribution à l'étude de la rotation résonnante dans le Système Solaire* (in French). Habilitation Thesis, URL <https://arxiv.org/abs/1502.01472> (2014)
- Noyelles B., Nimmo F.: New clues on the interior of Titan from its rotation state. In: *IAU Symposium, IAU Symposium*, vol **310**, pp 17–20 (2014)
- Peale S. J.: Generalized Cassini's Laws. *Astronom. J.* **74**, 483 (1969)
- Peale S. J., Margot J.-L., Hauck S. A., Solomon S. C.: Consequences of a solid inner core on Mercury's spin configuration. *Icarus* **264**, 443–455 (2016)
- Poincaré H.: Sur une forme nouvelle des équations de la mécanique. *Comptes rendus de l'Académie des Sciences* **132**, 369–371 (1901)
- Poincaré H.: Sur la précession des corps déformables. *Bulletin Astronomique* **27**, 321–357

- (1910)
- Rambaux N., Castillo-Rogez J.: Tides on Satellites of Giant Planets. In: Souchay J., Mathis S., Tokieda T. (eds) *Lecture Notes in Physics*, Berlin Springer Verlag, *Lecture Notes in Physics*, Berlin Springer Verlag, vol **861**, p 167 (2013)
- Rambaux N., Castillo-Rogez J. C., Le Maistre S., Rosenblatt P.: Rotational motion of Phobos. *Astron. Astrophys.* **548**:A14 (2012)
- Rappaport N., Bertotti B., Giampieri G., Anderson J. D.: Doppler Measurements of the Quadrupole Moments of Titan. *Icarus* **126**, 313–323 (1997)
- Richard A.: *Modèle de satellite à trois couches élastiques : application à la libration en longitude de Titan et Mimas* (in French). PhD thesis, Observatoire de Paris (2014)
- Richard A., Rambaux N., Charnay B.: Librational response of a deformed 3-layer Titan perturbed by non-Keplerian orbit and atmospheric couplings. *Planetary and Space Science* **93**, 22–34 (2014)
- Stiles B. W., Kirk R. L., Lorenz R. D., et al.: Determining Titan’s Spin State from Cassini RADAR Images. *Astronom. J.* **135**, 1669–1680 (2008)
- Stiles B. W., Kirk R. L., Lorenz R. D., et al.: Erratum: ”Determining Titan’s Spin State from Cassini Radar Images”. *Astronom. J.* **139**, 311 (2010)
- Vienne A., Duriez L.: TASS1.6: Ephemerides of the major Saturnian satellites. *Astron. Astrophys.* **297**, 588 (1995)
- Wang Y., Xu S.: Hamiltonian structures of dynamics of a gyrostat in a gravitational field. *Nonlinear Dynamics* **70**(1), 231–247 (2012)